DP-MS-78-9

CONF-780562--

EFFECTS OF RADIATIONS FROM TRANSURANIUM NUCLIDES ON CONTAINER SURFACES

by

W. R. McDonell and S. Dillich

Savannah River Laboratory
E. I. du Pont de Nemours and Co.
Aiken, South Carolina 29801

For presentation at the 8th Conference on Surface Studies, Savannah River Laboratory, Aiken, SC, May 9-11, 1978

DISCLAIMER

EFFECTS OF RADIATIONS FROM TRANSURANIUM NUCLIDES ON CONTAINER SURFACES*

by

W. R. McDonell and S. Dillich**

Savannah River Laboratory
E. I. du Pont de Nemours and Co.
Aiken, South Carolina 29801

ABSTRACT

Container materials for short-lived transuranium nuclides such as ^{242}Cm and ^{252}Cf may be implanted with sufficiently high concentrations of helium to cause surface blistering and other deleterious effects in some environments. Platinum and stainless steel surfaces adjacent to solid ^{242}Cm-oxide deposits showed no blisters after room-temperature exposures, but formed porous, distorted layers on postexposure heating. Platinum surfaces adjacent to solid ^{252}Cf-oxide deposits, in contrast, developed well-defined blisters with a variety of configurations during room-temperature exposures. Formation of the blisters at low temperatures was attributed to the fission-fragment-induced agglomeration of implanted helium, coupled with a stress-relieving

* The information contained in this article was developed during the course of work under Contract No. AT(07-2)-1 with the U.S. Department of Energy.

** Present address: Dept. of Materials Science, Engineering School, Univ. of Virginia, Charlottesville, VA 22903.

transport of atoms displaced by fission fragments into the blister walls. High-temperature exposures produced less well-defined globular protrusions at much lower concentrations of implanted helium.

Immersion of glass or platinum specimens in dilute ^{242}Cm or ^{252}Cf solutions caused no significant surface damage, and on subsequent reaction with acidic or caustic reagents other than HF, the surfaces displayed no well-defined effect of the radiation exposures. HF solutions preferentially etched fission tracks in ^{252}Cf-exposed glass specimens. No significant retention of ^{252}Cf implanted in container surfaces by fission fragment impact was detected.

INTRODUCTION AND SUMMARY

Container materials for short-lived transuranium nuclides such as ^{242}Cm and ^{252}Cf may be implanted with sufficiently high concentrations of helium to cause surface blistering and other deleterious effects in some environments.[1,2,4] Alpha decay of such nuclides over times approximating their half-lives (163 days for ^{242}Cm, 2.65 years for ^{252}Cf) implants helium in adjacent surfaces up to 3 atom %; spontaneous fission of the ^{252}Cf produces in addition a concurrent high displacement of lattice atoms (typically 100 displacements per atom). This paper is a report on the status of studies conducted at the Savannah River Laboratory to characterize the surface effects of exposure of typical container materials to ^{242}Cm and ^{252}Cf radiations under several processing, storage, and use conditions. Most severe effects were expected to be produced by exposures of container materials to dense, solid forms of the nuclides during storage and use. Direct effects of exposure of container materials to relatively dilute solutions of the nuclides employed during processing were not expected to be severe, but might be complicated by chemical attack of processing reagents on the exposed materials.

We found, in summary, that platinum and stainless steel surfaces exposed to solid ^{244}Cm oxide over about two half-lives suffered no evident deterioration at low temperatures, but formed porous and distorted surface layers on subsequent heating to above 1000°C. On the other hand, platinum alloy surfaces exposed to solid ^{252}Cf oxide over about one half-life developed well-defined blisters in a variety of configurations at low temperature. Formation of the blisters was attributed to the fission-fragment-induced agglomeration of implanted helium, coupled with a stress-relieving transport of atoms displaced by the fission fragments into the blister walls. High-temperature exposures produced less-well-defined globular protrusions at much lower concentrations of implanted helium.

Finally, the immersion of glass or platinum specimens in dilute ^{242}Cm or ^{252}Cf solutions caused no significant surface damage over the short times required for normal aqueous processing of the nuclides. On subsequent reaction of the container materials with acidic or caustic reagents other than HF, the surfaces were not greatly affected by either ^{242}Cm or ^{252}Cf radiation exposures.

HF solutions preferentially etched fission fragment tracks in ^{252}Cf-exposed glass specimens. No significant retention of ^{252}Cf implanted in container surfaces by fission fragments impact was detected.

SURFACE EFFECTS OF ALPHA PARTICLES FROM SOLID ^{244}Cm OXIDE

The extent of surface deterioration of container materials implanted with high concentrations of helium was investigated by exposing typical materials, platinum and stainless steel, to alpha particles from solid ^{242}Cm-oxide deposits.[1] The ^{242}Cm, an alpha-emitting nuclide with half-life of 163 days, was used to simulate ^{252}Cf alpha radiations without a concurrent fission fragment exposure. The platinum specimens were thin metal disks exposed to a 50% pure ^{242}Cm-oxide deposit within two stainless steel cups (Slide 1). As previously described, 5-mg quantities of the ^{242}Cm were transferred to the cups as an oxalate slurry, where it was dried and in one case calcined in-place to the oxide at 500°C. During subsequent storage for about 300 days at room temperatures, the platinum disks above the ^{242}Cm deposits were exposed to about 5×10^{17} alpha particles/cm^2, as estimated geometrically, and surfaces of the stainless steel cups adjacent to the deposits were exposed to about 3×10^{18} alpha particles/cm^2. Corresponding concentrations of implanted helium decreased nearly linearly from maximum values of about 1 atom % for the platinum disks and up to 5 atom % for the stainless steel cups at the specimen surfaces to zero at the maximum depth of penetration of the 6.1-MeV alpha particles (10-15 μm) (Slide 2).

No major surface deterioration was observed on either the platinum disks or the rough-machined stainless steel cups after the room-temperature exposure; the exposed surfaces were free of blisters. On subsequent heating, however, both materials developed porous distorted surface layers. The platinum disks heated to above 1400°C exhibited irregularly shaped blisters ranging up to 20 μm in size (Slides 3a and 3b). Metallographic cross sections showed the blisters were caused by agglomeration of helium into a few relatively large (1-10 μm) gas bubbles at grain boundaries within a 10-μm thick surface layer of the specimen (Slide 4).

High-Temperature Blistering

Development of the distorted surface layer on one platinum disk was characterized as a function of temperature using scanning electron microscopy. From room temperature to about 800°C, the specimen surfaces were distinguished only by black marks or grooves at grain boundaries, which became more prominent with increased temperature; both exposed and unexposed areas of the disk surface exhibited these marks (Slides 5 and 6). Above 800°C, the grain-boundary marks were resolved into a series of discrete pores, which increased in size up to 2-3 μm at 1400°C (Slide 7). At 1400°C also, thermal etching produced a contouring of grain surfaces and relief of grain boundaries in both exposed and unexposed areas. Heating at 1600°C, however, produced a well-defined convolution of the surfaces in exposed areas of the disk, accompanied by the formation of large (5 μm) grain-boundary holes (Slides 8 and 9). Unexposed regions exhibited only thermal contouring of the grain surfaces and edges, and the grain-boundary pores were less than one-tenth the size of the holes in the exposed region, an apparent decrease over their 1400°C dimensions.

The exposed surfaces of the stainless steel cups exhibited analogous, but more pronounced effects on heating. No major deterioration of the bottom of the cups was evident before heating; minor erosion of the machine-marked surface compared to an unexposed blank was probably caused by chemical corrosion (Slides 10 and 11). Heating in air at 800°C produced no blistering, although the surface of the exposed cups tarnished more than the blank cup. Heating at 1000°C and 1200°C, however, eliminated the machine markings on the exposed surfaces and formed a featureless black surface contrasted to the oxidized but still machine-marked surface of the blank cup (Slide 12). Cross sections of the exposed cup showed a porous surface layer about 15-μm thick with helium agglomerated into many small (∿1 μm) bubbles (Slide 13). No well-defined gradient in bubble size or frequency corresponding to the expected decrease in helium concentration with depth of implantation was evident; stringers of fairly large bubbles at the interface of the porous layer and the solid unimplanted metal were sometimes seen. The uniformity of bubble sizes suggested that availability of vacancies rather than helium concentration governed bubble growth within the implanted layer; the large interface bubbles benefited by agglomeration of vacancies from the adjacent unimplanted metal. No significant spalling of the porous layer occurred, although metallographic sectioning produced a gap which indicated that the porous layer could be mechanically separated from the solid metal (Slide 14).

The results of the ^{242}Cm exposures were generally in accord with previous observations suggesting that concentrations of implanted helium exceeding about 20% were required for blistering of material surfaces at low temperatures.[3] It was concluded that the alpha-emitting radionuclides generally should produce no major surface distortion of container materials due to blistering at low temperatures. Moreover, the porous surface layer formed at high temperature released implanted helium without a detrimental spalling of the capsule material.

SURFACE EFFECTS OF ALPHA PARTICLES AND FISSION FRAGMENTS FROM SOLID ^{252}Cf OXIDE

Californium-252, which decays with a 2.65-year half-life (97% by alpha emission and 3% by spontaneous fission), is encapsulated at the Savannah River Laboratory for use as a neutron source.[5] Surface effects of the ^{252}Cf radiations were characterized by destructive examination of the Pt-10% Rh capsule of a source containing initially 17.8 mg ^{252}Cf and used for about two years near room temperature in an activation analysis facility.[2] The ^{252}Cf was contained as a 30% pure oxide deposit between two porous platinum filters within the capsule (Slide 15). Decay of the ^{252}Cf exposed adjacent surfaces to about 1.2×10^{18} alpha particles/cm^2 and implanted helium in concentrations ranging from about 3 atom % at the capsule surface to zero at the maximum depth of penetration of the 6.1-MeV alpha particle, about 12 μm (Slide 16). The capsule surfaces were concurrently exposed to 4×10^{16} fission fragments/cm^2, which produced lattice damage ranging from about 100 displacements per atom at the capsule surface to zero at a depth equal to the maximum fission fragment range (about one-half the alpha particle range).[6] The concentrations of implanted helium were much less than the 20 atom % or more required to produce blistering at low temperatures by alpha particles or accelerator helium ions alone.[3]

Low-Temperature Blistering

Examination of capsule surfaces in the scanning electron microscope, after recovery of ^{252}Cf and cleaning in concentrated nitric acid, revealed many small blisters with various configurations in areas extending from just above the bottom filter to about 4 mm up the capsule wall. The areal density of the blisters was in the range 10^6 to 10^7/cm^2. Areas under the filters were free of blisters (Slide 17a).

The size and shape of the blisters depended on their location. Just above the bottom filter, the blisters displayed circular cross sections ranging between 1 and 10 μm in diameter, and emerged the same or greater distances from the capsule surfaces to form ellipsoidal balloons (Slide 17b). The thickness of the blister walls appeared no greater than a few tenths of a micrometer.

Areas farther away from the bottom filter displayed characteristically elongated blisters, preferentially aligned parallel to the capsule length (Slide 18). Farthest from the filter, *vertically elongated* filament-like blisters were connected to the capsule surface at one end only. These blisters, with approximately circular bases, were about 1 μm in diameter and up to 10 μm in length. Their free ends were generally directed away from the filter, and they sometimes overlapped in tangled arrays. At intermediate distances, *laterally elongated* blisters with elliptically shaped bases were connected to the capsule surface over most of their length. The laterally elongated blisters were generally shorter and wider than the vertically elongated blisters, but in some areas were found in parallel arrays extending lengthwise 50 to 100 μm or more (Slide 19).

Near the top filter, both circular and laterally elongated blisters were observed in interrelated patterns (Slide 20).

Spalling of surface layers in some areas produced occasional bare spots ranging in size from 10 to 100 μm (Slide 21a). Laterally elongated blisters surrounding the bare spots exhibited distinctive flow patterns (Slide 21b). Some areas of the capsule surface were abrasively scraped clean of blisters, probably during movement of the top filter during sectioning of the capsule (Slide 22a). Where such regions traversed a circumferential machine mark, the recessed area showed characteristic blisters. Surface protrusions produced adjacent shadowed regions of fewer blisters, and the protrusions themselves exhibited blisters of various configurations (Slide 22b).

Cross sections of blistered areas examined by optical microscopy revealed no resolvable subsurface bubbles. The blistering affected only an unresolvable thin layer of surface material. The ^{252}Cf capsule suffered no obvious deterioration in containment integrity.

Mechanism of Low-Temperature Blistering

The unique features of the blisters produced by ^{252}Cf exposures at low temperatures were attributed to interactions of implanted helium with lattice defects, e.g. vacancies and interstitial atoms produced by the fission fragments (Slide 23). Helium implantation generates a lateral compressive stress in the surface layer of an exposed material, because of the restraints on expansion of the implanted layer by the underlying metal.[8] The helium atoms, with mobility enhanced by fission fragment impacts, agglomerate along with the vacancies to form helium bubbles in near-surface regions of the exposed material,[9] leaving residual interstitial atoms around the bubble to agglomerate into dislocation loops specially oriented to relieve the lateral compressive stresses. Glide of the interstitial loops under these stresses to the surface displaces successive layers of lattice atoms to form the blister walls. This mechanism is analogous to that postulated for growth of metallic whiskers on certain electroplated metal surfaces.[10] The mechanism suggests that reciprocally critical values of lateral stress and bubble size are necessary for blister nucleation. Since lateral stress depends principally on concentration of implanted helium and bubble size depends (at low temperatures) on the number of atoms displaced by the fission fragments, blistering in a high-displacement environment occurs at a relatively low implanted helium concentration.

The varying configurations of the blisters along the capsule wall result from radiation intensity gradients produced by the ^{252}Cf source located principally on the bottom filter. Helium implanted by alpha particles and atoms displaced by fission fragments decrease with distance from the radiation source but the helium-to-displaced-atom ratio increases (because the alpha particles have a greater range than the fission fragments). The circular blisters near the bottom filter form in regions of relatively uniform helium and displaced atom concentrations; the blisters nucleate uniformly and grow laterally in symmetrical configurations. In contrast, the elongated blisters farther from the filter develop in more-or-less pronounced helium and displaced atom gradients. Movement of the blister front up the capsule wall produces the laterally elongated blisters in intermediate regions of the capsule surface. The increase in helium-to-displaced-atom ratio, which promotes vertical growth over lateral growth of the blisters, produces the vertically elongated blisters in regions of the capsule surface farthest removed from the radiation source.

High-Temperature Blistering

The effects of ^{252}Cf radiations on container surfaces at high temperatures were characterized on two capsules heated for 6000 hours at 1000°C. The capsules had initially contained, as oxide deposits, 170 mg ^{252}Cf in 810 mg of praseodymium carrier and 163 mg ^{252}Cf in 846 mg of samarium carrier, respectively. Exposures of adjacent capsule surfaces during the high-temperature test to about 1.5×10^{17} alpha particles/cm^2 implanted helium in maximum concentrations of about 0.4 atom % at the capsule surface. Corresponding fission fragment exposures of about 5×10^{15} fragments/cm^2 produced a maximum 12 displacements per atom at the capsule surface.

Visual examination of capsule sections, after recovery of the ^{252}Cf and cleaning in concentrated nitric acid, showed a clean but irregular inner surface between the location of the platinum filters, with only minor variations in shading along the capsule length (Slide 24). Examination in the scanning electron microscope revealed the surface to be covered with globular protrusions interspersed with large holes, in contrast to the contoured but relatively smooth surface under the filters (Slide 25). Although some variation in severity of distortion between the filters was apparent, the whole surface exhibited the same type of irregularity. The globular protrusions had generally the same lateral dimensions (10-20 μm) as the convolutions produced by heating ^{242}Cm-exposed surfaces, but were vertically much more pronounced. The holes produced in the two cases were about the same size, however. The grain size of the distorted metal between the filters of the ^{252}Cf capsule was about the same as the lateral dimensions of the protrusions, but was much smaller than the 50-150 μm grain size of the metal under the filter; the helium implanted between the filters evidently inhibited grain growth over long times at high temperatures in this region.

The mechanism of distortion of ^{252}Cf-exposed surfaces at high temperature is presumably related to the mechanism for surface blistering at low temperature. The holes in the porous surface are produced by agglomeration of helium along with vacancies into gas bubbles and the globular protrusions are produced by deposition of atoms displaced by the fission fragments into special configurations. Analogous distortions caused by fission fragments in uranium are known to persist up to equivalent temperatures ($0.6\ T_m$).[11] The surface distortions occur at high temperatures at much lower concentrations of implanted helium than at low temperature because of the greater mobility of both helium and vacancies at high temperatures. The relative uniformity of the surface distortion along the capsule length at high temperatures, in contrast to that at low temperatures, is attributed either to a uniform deposition of the ^{252}Cf deposit on the capsule walls over the long times at high temperatures, or to the low thresholds of implanted helium required for high temperature distortion, readily exceeded by exposures of all capsule surfaces within the range of the alpha particle and fission fragment radiations.

In addition, some surface distortions produced in ^{252}Cf capsules at high temperature may be caused by thermal evaporation and redeposition of surface metal within the capsules.

EFFECTS OF ^{242}Cm AND ^{252}Cf SOLUTIONS ON CONTAINER MATERIAL SURFACES

Surface effects of radiations from ^{242}Cm and ^{252}Cf in aqueous media were investigated by immersion of representative glass and metal specimens in dilute solutions of the nuclides. Although the direct effects of such low-intensity radiation would be minor, the radiations could accelerate erosion caused by chemical attack of the materials in common process reagents.

^{242}Cm Alpha Particle Exposures

To evaluate the extent of surface damage induced by alpha radiation alone, soda-lime glass slides (Esco No. 2950-F) and borosilicate glass plates (Corning No. 7740) were immersed along with unalloyed platinum disks for up to 36 days in 0.3N HNO_3 solutions containing 30 μg/ml ^{242}Cm. This exposed the surfaces of the samples to about 1.5×10^{13} alpha particles/cm^2 (assuming a 50-μm range for the alpha particles in water) and implanted helium in concentrations ranging from a maximum of about 10^{-5} atom % at the specimen surface to zero at the maximum depth of penetration of the alpha particles into the specimen surfaces.

No deterioration of either glass or platinum specimen surfaces was evident after exposure, although the glass specimens were somewhat discolored (Slides 26 and 27). Subsequent immersion of the glass specimens in conc HNO_3 (30 min), 6N HCl (30 min), aqua regia (90 min), and 6N KOH (30 min) produced no surface effect discernible by optical microscopy (Slides 28, 29, 30, and 31). The glass specimens did etch in 5% HF, however, to reveal a few fission fragment tracks produced by a low level of spontaneous fission in ^{242}Cm (Slides 32a and 32b). The platinum specimens were similarly unaffected by conc HNO_3 (60 min) and 6N HCl (30 min); they did etch, however, in aqua regia (70 min), but without significant effect of ^{242}Cm exposure (Slide 33). It was concluded that the alpha particle radiation from ^{242}Cm in aqueous solution would not significantly erode glass or platinum container vessels over the short times required for normal chemical processing.

^{252}Cf Alpha Particle and Fission Fragment Exposures

Silicon is a persistent and troublesome impurity in ^{252}Cf solutions thought to result from fission-fragment-induced erosion of glass vessels. To evaluate concurrent effects of alpha-particle and fission fragment radiations on glass vessels, a soda-lime glass slide was immersed at one end in a 0.1N HNO_3 solution containing 133 μg/ml ^{252}Cf. In the test, the specimen surfaces were exposed to about 2×10^{11} alpha particles/cm^2 and implanted with helium at a maximum concentration of about 10^{-7} atom %. Corresponding fission fragment exposure was about 10^{10} fragments/cm^2, which produced a maximum 2×10^{-5} displacements per atom in the specimen surface.

No well-defined surface damage attributable to the ^{252}Cf exposure was evident on the glass slide by optical microscopy.

Although the immersed end of the slide showed a somewhat greater incidence of surface pits, such features were very nonuniformly distributed over the specimen and no demarkation between the ^{252}Cf-exposed and unexposed areas could be seen (Slide 34).

Subsequent digestion of the specimen in a series of processing reagents also revealed no well-defined effect of the ^{252}Cf exposure, although several of the reagents appeared to attack the exposed end of the slide somewhat more than the unexposed end. Digestion in conc HNO_3 over 4 days, for example, produced patterns in the ^{252}Cf-exposed area not seen in the unexposed area (Slide 35). Overnight digestion in 6N KOH produced a nonuniform etching also possibly more pronounced in the ^{252}Cf-exposed area than in the unexposed area, but not definitely so because of a nonuniform attack (Slide 36). Immersion in 6N HCl (1 hr) and in aqua regia (1 hr) had no additional effect. On the other hand, HF either as a trace addition (0.03N) to conc HNO_3 or as a 5% aqueous solution did preferentially attack the ^{252}Cf-exposed areas (Slide 37). Severity of the attack was such that individual fission fragment tracks were resolved only at the interface between the exposed and unexposed areas, where fragments that escaped the surface of the ^{252}Cf solution were recorded (Slide 38). The ^{252}Cf-exposed areas dissolved fairly uniformly and at a demonstrably higher rate than unexposed areas; this sensitization to preferential dissolution persisted to depths far below the fission fragment range. The texture of the etched surface in exposed and interface areas coarsened as etching proceeded, with the interface areas evidencing larger pits than the more-uniformly etched exposed areas (Slides 39 and 40).

It was concluded that the alpha-particle and fission-fragment radiations from ^{252}Cf should not, over short times, markedly deteriorate the surfaces of glass vessels, except in HF solutions. Further evaluation of the minor erosion effects observed and the consequent introduction of impurity silicon into process solutions will require more sensitive characterization techniques.

^{252}Cf RETENTION ON CONTAINER SURFACES

Comparison of ^{252}Cf retention in platinum shipping containers held for more than two years before ^{252}Cf recovery with that of promptly recovered containers showed no significant reduction in recovered product because of implantation of ^{252}Cf in the container surfaces under fission fragment impact. The shipping containers were prepared at ORNL by calcination of ^{252}Cf-loaded ion-exchange resin; the ^{252}Cf was recovered at SRL by elution with 0.1N HNO_3. Recovery data are summarized in Slide 41.

REFERENCES

1. W. R. McDonell. "Surface Blistering of Materials Exposed to ^{242}Cm Radiations." *ANS Trans. 21,* 135 (1975).

2. W. R. McDonell. "Fission-Fragment-Induced Helium Blistering of ^{252}Cf-Exposed Surfaces." *ANS Trans. 27,* 271 (1977).

3. G. J. Thomas and W. Bauer. "Helium Implantation Effects in Palladium at High Doses." *Radiat. Eff. 17,* 221 (1973).

4. S. K. Das and M. Kaminsky. "Radiation Blistering in Metals and Alloys." p. 112 in *Radiation Effects on Solid Surfaces* (Advances in Chemistry Series 158). M. Kaminsky, Ed., American Chemical Society, Washington, D. C. (1976).

5. A. R. Boulogne and J. P. Faraci. "Californium-252 Neutron Sources for Industrial Applications." *Nucl. Technol. 11,* 75 (1971).

6. T. H. Gould and W. R. McDonell. "Radiation Damage by ^{252}Cf Fission Fragments and Alpha Particles." p. 387 in *Radiation Effects and Tritium Technology for Fusion Reactors* (Proceedings of Int. Conf. held at Gatlinburg, Tenn., Oct. 1-3, 1975). USERDA Report CONF-750989 Vol. II, Oak Ridge National Laboratory, Oak Ridge, Tenn. (1976).

7. W. R. McDonell. "Whisker Growth - A New Mechanism for Helium Blistering of Surfaces in Complex Radiation Environments." *3rd International Conference on Plasma Surface Interactions in Controlled Fusion Devices, Culham Laboratory, Abingdon, England, April 3-7, 1978. J. Nucl. Mater.* (to be published).

8. E. P. EerNisse and S. T. Picraux. "Role of Integrated Lateral Stress in Surface Deformation of He-Implanted Surfaces." *J. Appl. Phys. 48*(1), 9 (1977).

9. D. J. Mazey, B. L. Eyre, J. H. Evans, S. K. Events, and G. M. McCracken. "A Transmission Electron Microscopy Study of Molybdenum Irradiated with Helium Ions." *J. Nucl. Mater. 64,* 145 (1977).

10. U. Lindborg. "A Model for the Spontaneous Growth of Zinc, Cadmium, and Tin Whiskers." *Acta Met. 24,* 181 (1976).

11. W. R. McDonell. "Void Model for Cavitational Swelling of Uranium." p. 266 in *Physical Metallurgy of Reactor Fuel Elements* (Proceedings of International Conference, Berkeley, England, September 2-7, 1973). J. E. Harris and E. C. Sykes, Eds., The Metals Society, London (1975).

SLIDE 1
CAPSULE FOR EXPOSING PLATINUM DISKS
TO ^{242}Cm ALPHA RADIATIONS

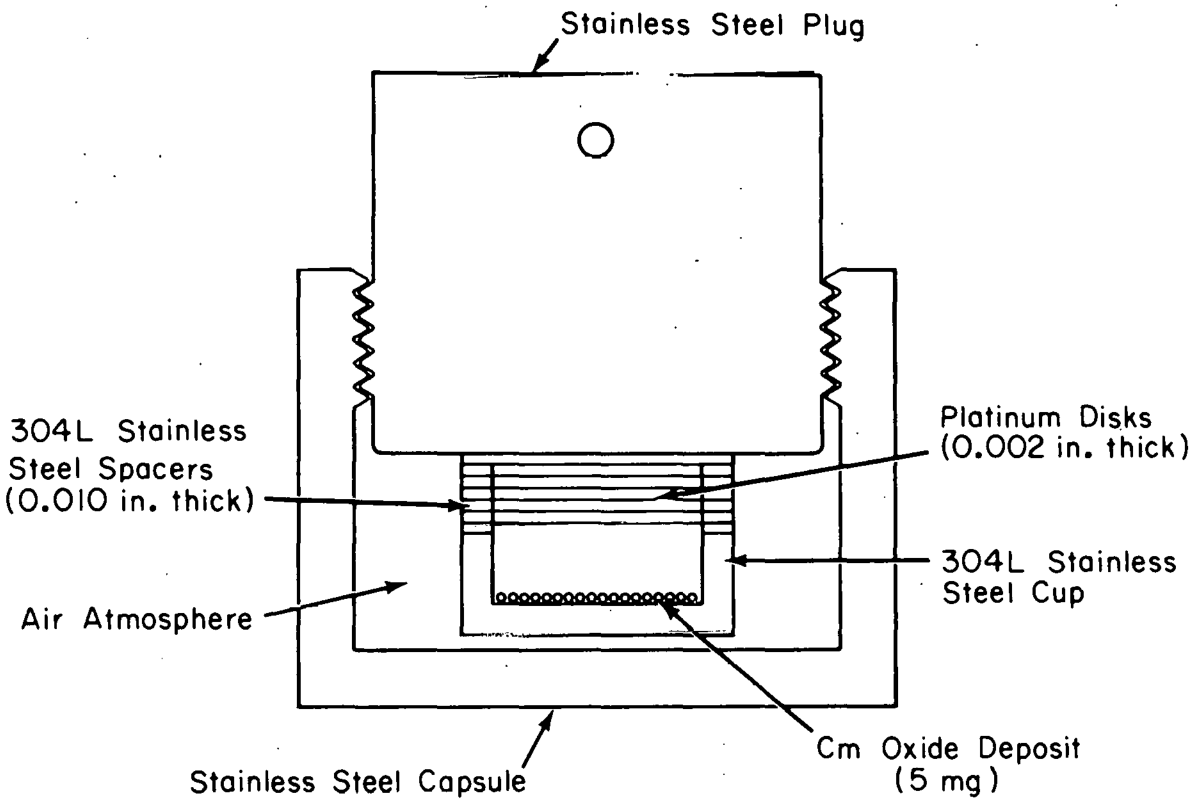

SLIDE 2

HELIUM CONCENTRATION DISTRIBUTION IN SOURCE AND CONTAINER MATERIALS

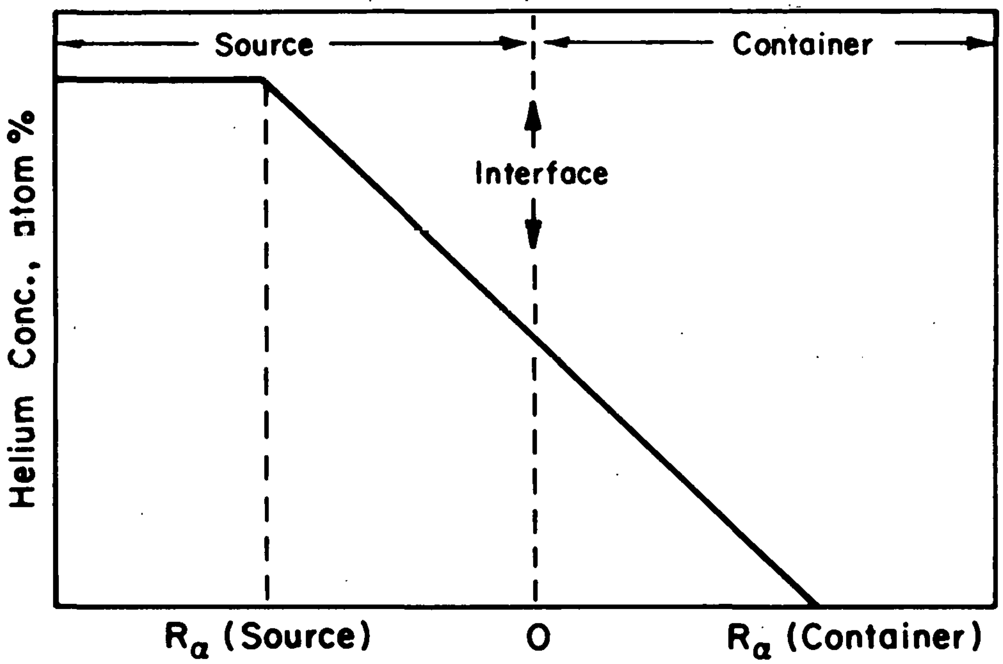

^{242}Cm 6.1-MeV ALPHA PARTICLES (Range in $^{242}Cm_2O_3$ ~13 μm)

	Platinum	Stainless Steel
Range, μm	10	15
Max Exposure, particles/cm^2	5×10^{17}	3×10^{18}
Max He Conc., atom %	~1	~5

SLIDE 3A

^{242}Cm ALPHA-IRRADIATED PLATINUM DISK AFTER 1500°C HEATING

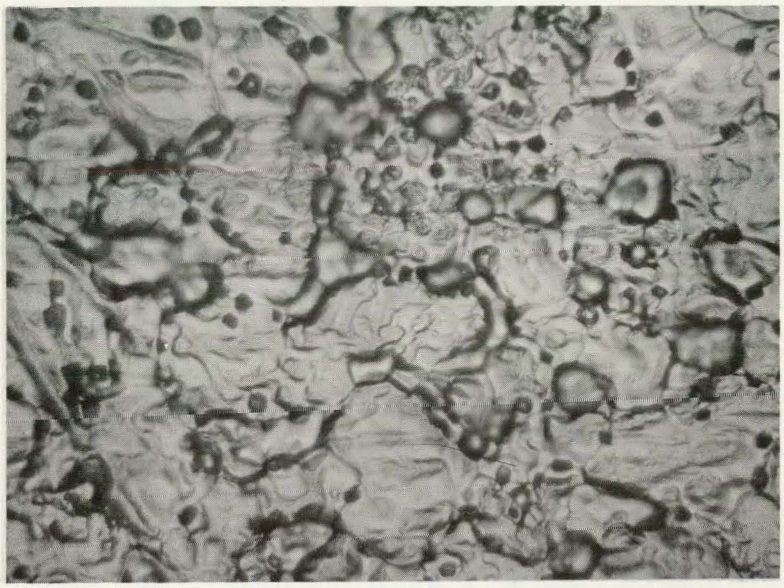

Exposed Side - Grain Boundary Blisters

40 μm

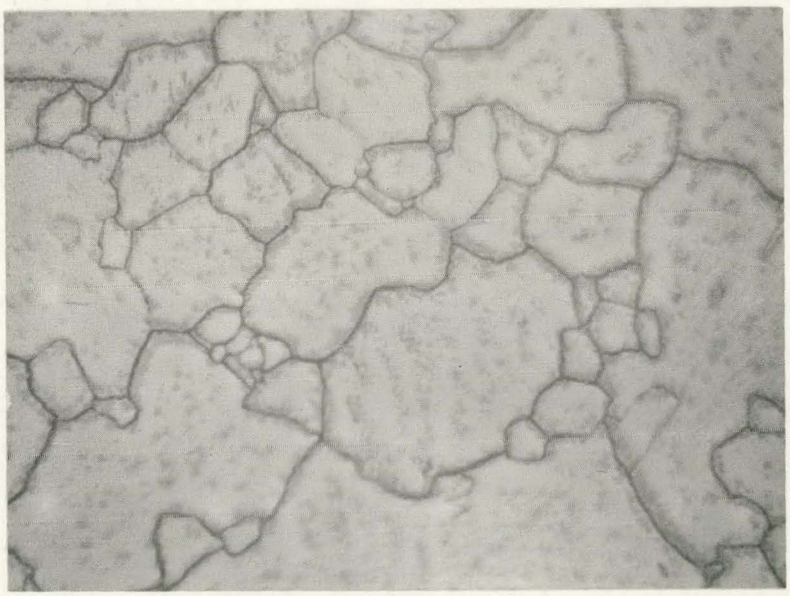

Unexposed Side - Thermally Etched Grain Boundaries

SLIDE 3B

^{242}Cm ALPHA-IRRADIATED PLATINUM DISK AFTER 1500°C HEATING

Exposed Side - Helium Blisters

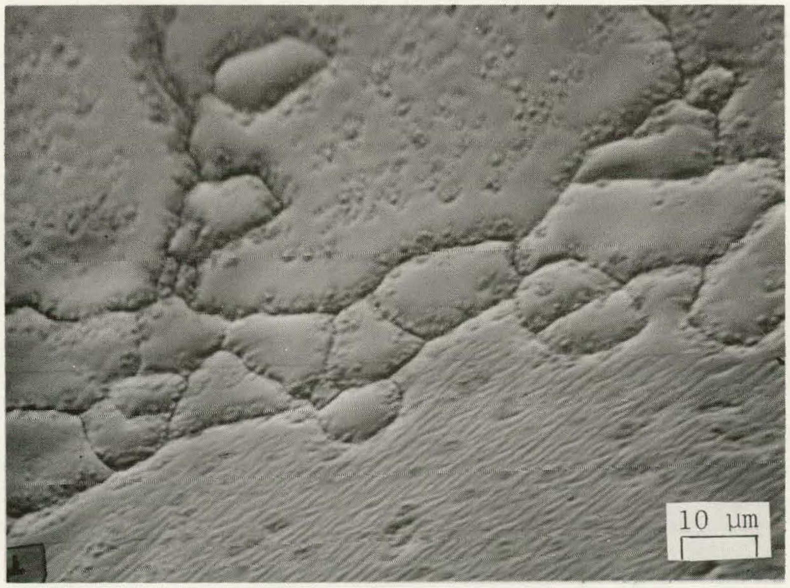

Unexposed Side - Thermally
Etched Grain Boundaries

SLIDE 4

IA IRRADIATED PLATINUM DISK AFTER 1500°C HEATING

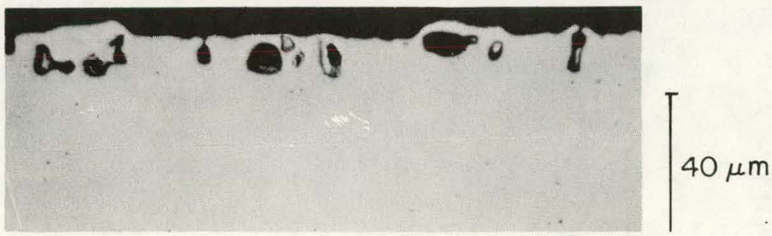

e. Heated 1200°C, 4 hr

SLIDE 5

EFFECT OF HEATING ON SURFACES OF ^{242}Cm-EXPOSED PLATINUM DISK

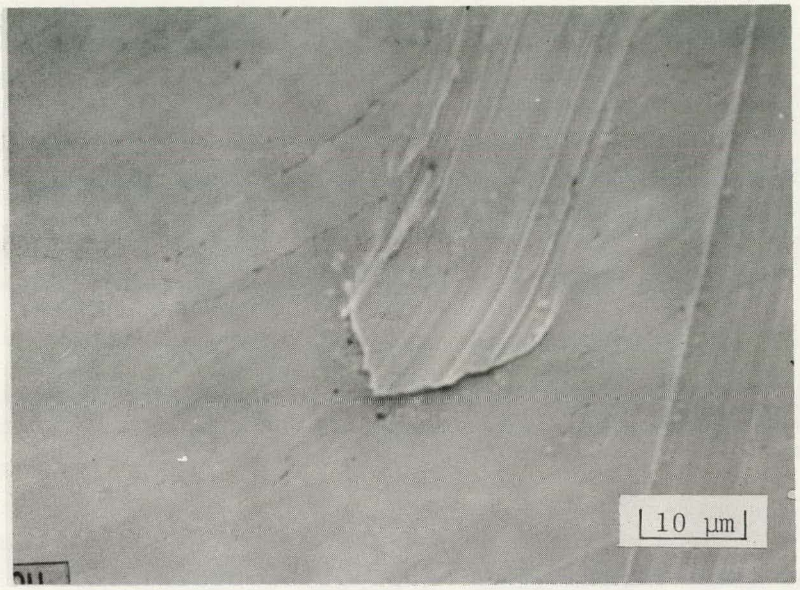

a. Unheated

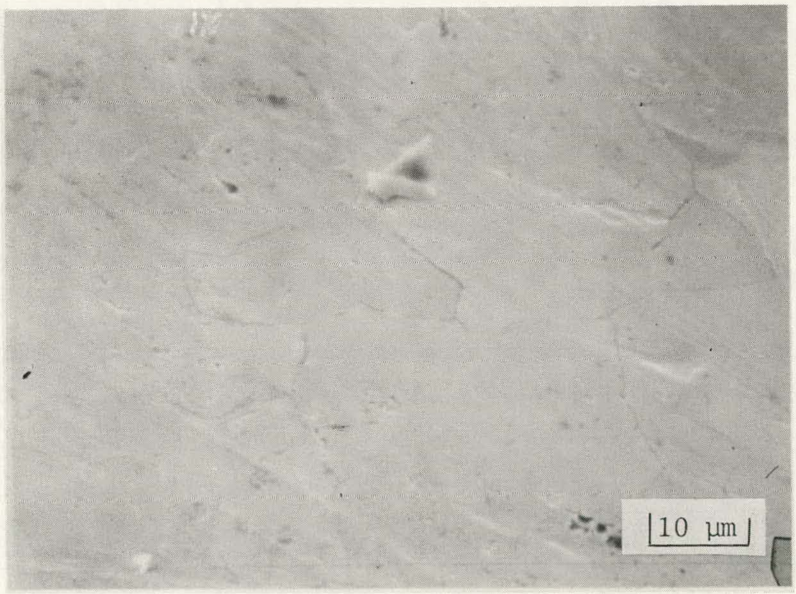

b. Heated 500°C, 4 hr

SLIDE 6

EFFECT OF HEATING ON SURFACES OF ^{242}Cm-EXPOSED PLATINUM DISK (CONT'D)

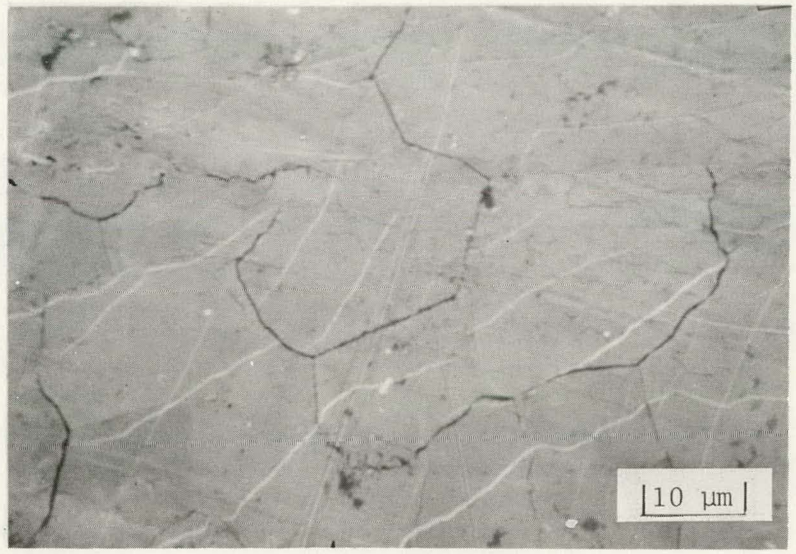

c. Heated 800°C, 4 hr

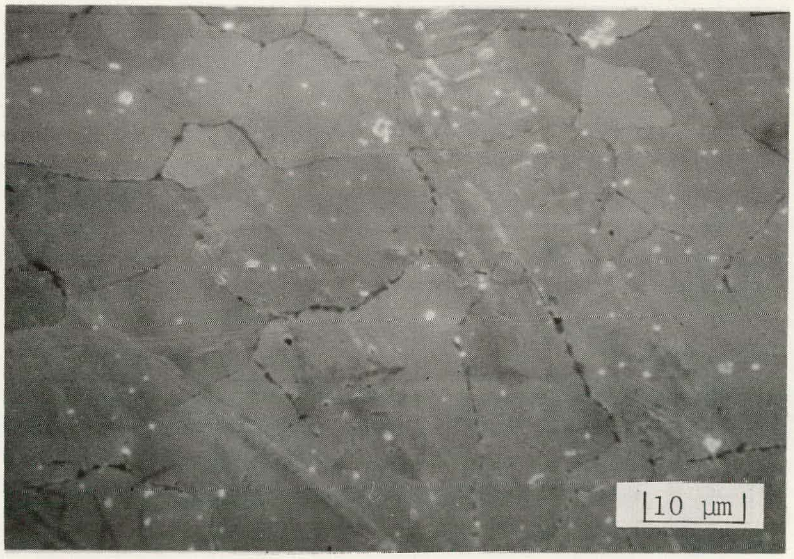

d. Heated 1000°C, 4 hr

SLIDE 7

EFFECT OF HEATING ON SURFACES OF ^{242}Cm-EXPOSED PLATINUM DISK (CONT'D)

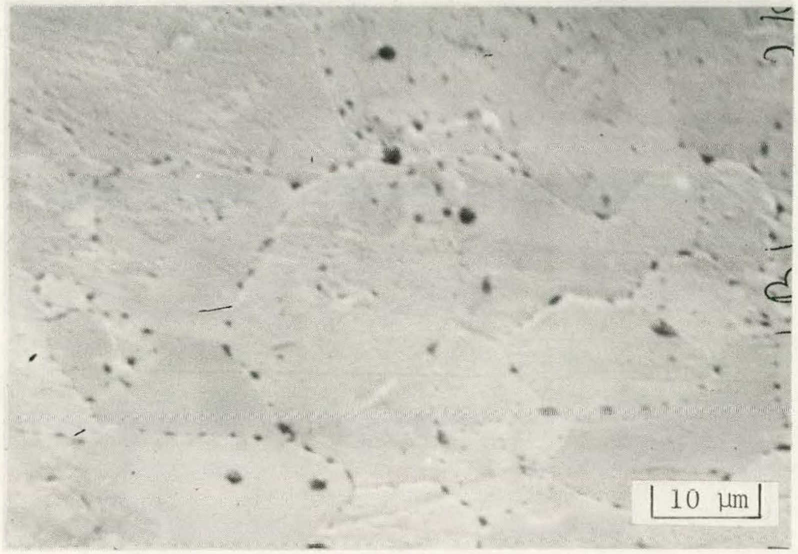

e. Heated 1200°C, 4 hr

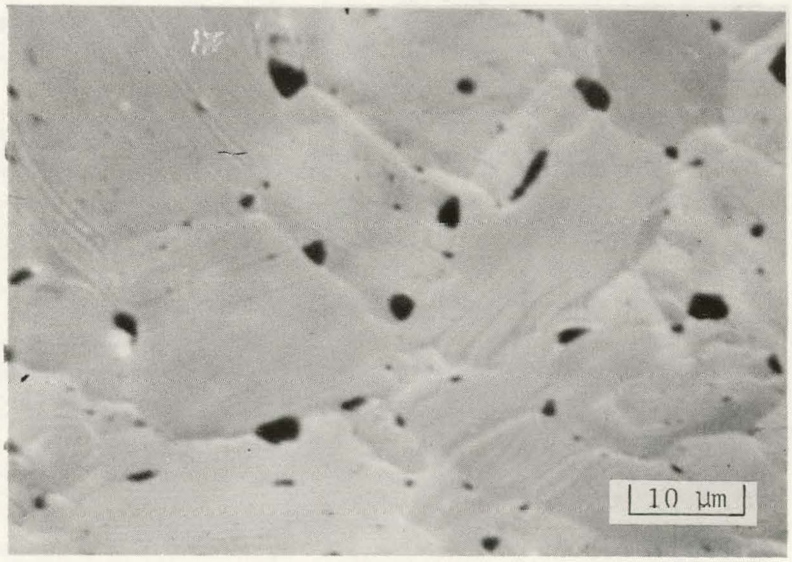

f. Heated 1400°C, 4 hr

SLIDE 8

EFFECT OF HEATING ON SURFACES OF ^{242}Cm-EXPOSED PLATINUM DISK (CONT'D)

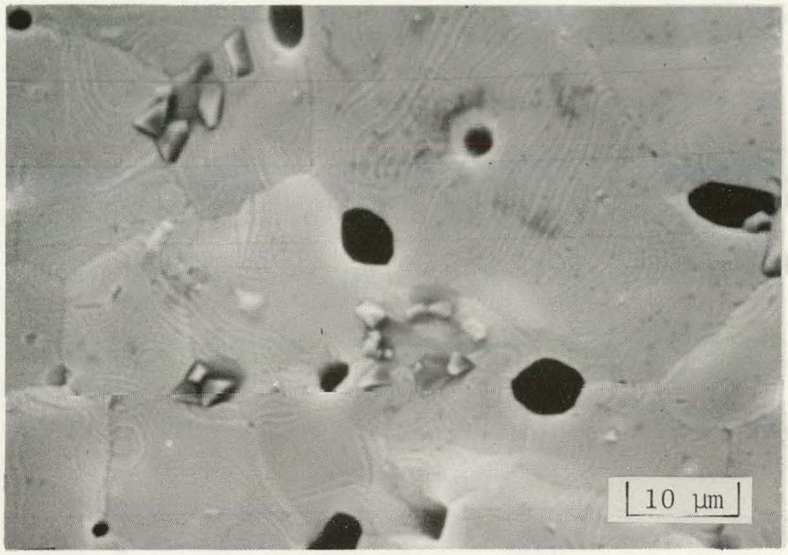

g. Exposed Area, Heated 1600°C, 4 hr

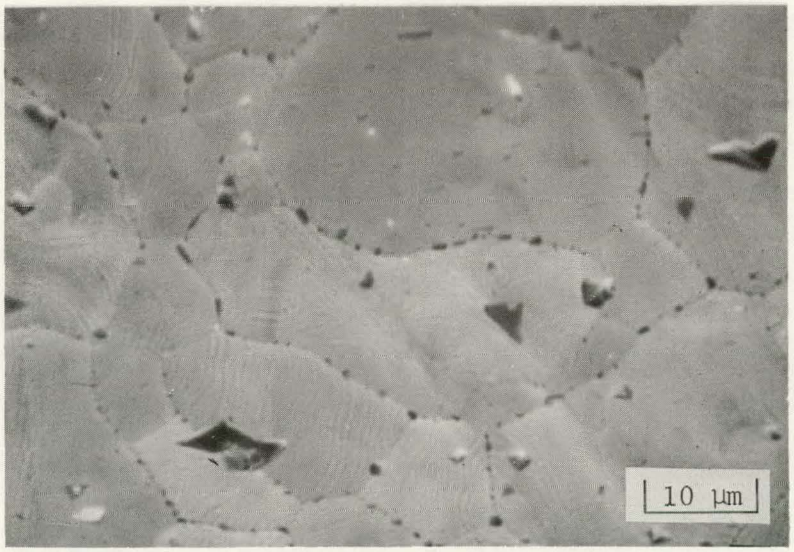

h. Unexposed Area, Heated 1600°C, 4 hr

SLIDE 9

INTERFACE BETWEEN ^{242}Cm-EXPOSED AND UNEXPOSED AREAS ON PLATINUM DISK

Heated 1600°C, 4 hr

SLIDE 10

^{242}Cm-EXPOSED 304L STAINLESS STEEL CUP BEFORE HEATING

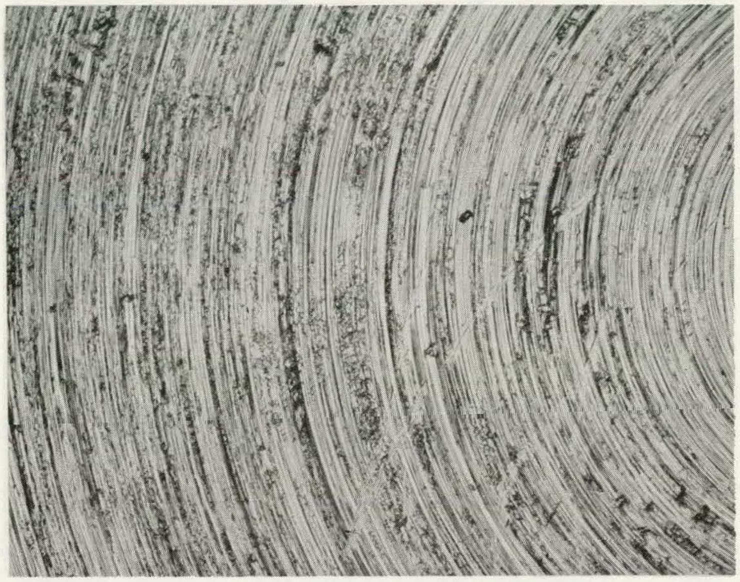

Unexposed Blank

200 μm

As-Exposed Surface

SLIDE 11

^{242}Cm-EXPOSED 304L STAINLESS STEEL CUP BEFORE HEATING

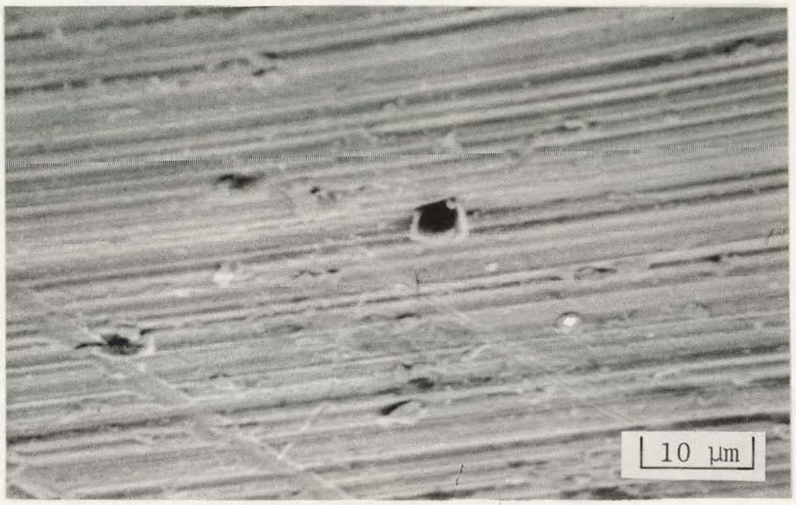

SLIDE 12

^{242}Cm-EXPOSED 304L STAINLESS STEEL CUP AFTER HEATING 1000°C

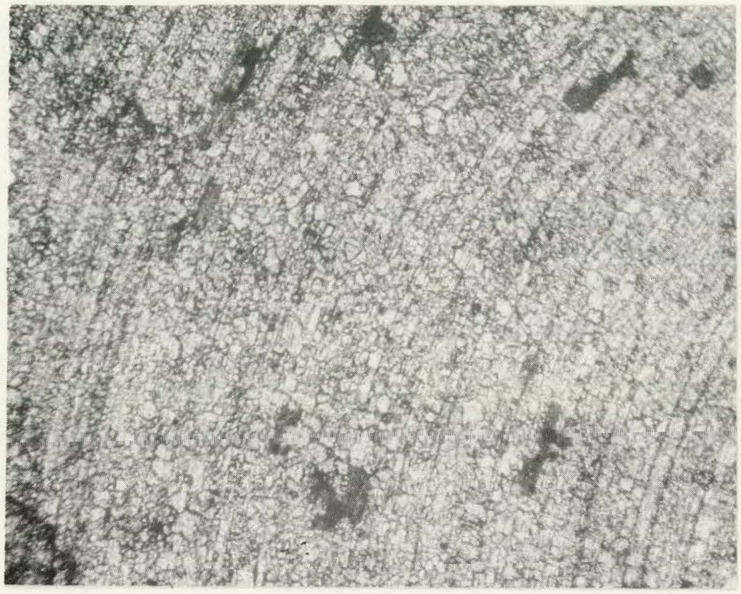

Unexposed Blank

200 μm

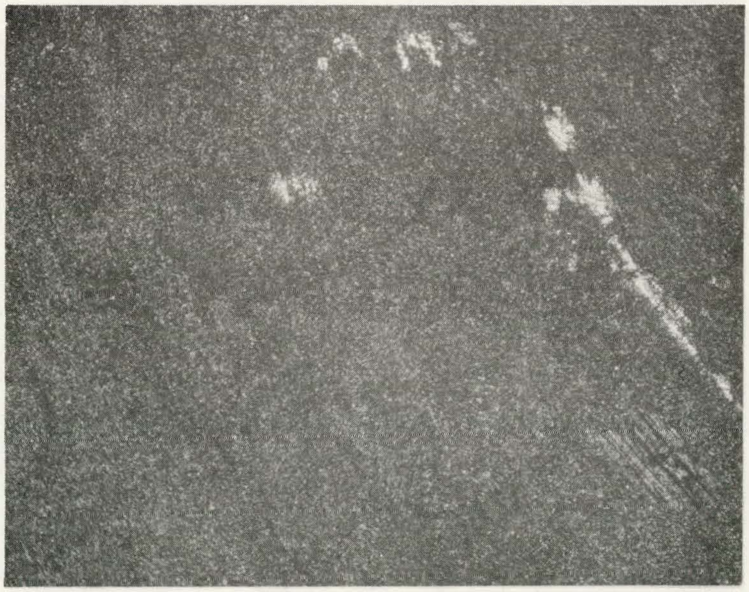

Exposed Surface

SLIDE 13

^{242}Cm-EXPOSED 304L STAINLESS STEEL CUP
BEFORE AND AFTER HEATING AT 1000°C

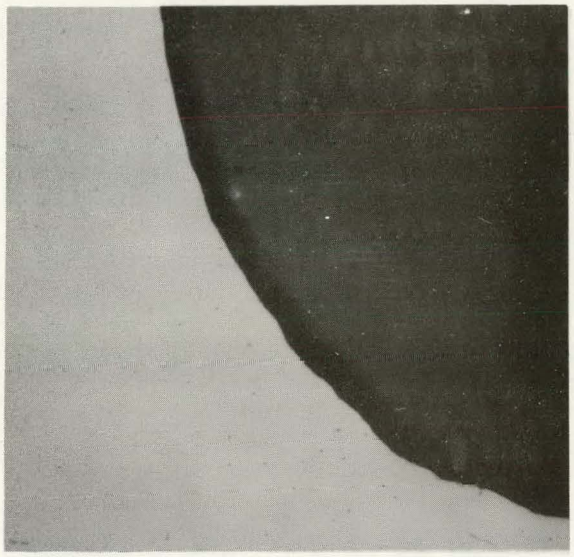

Before Heating

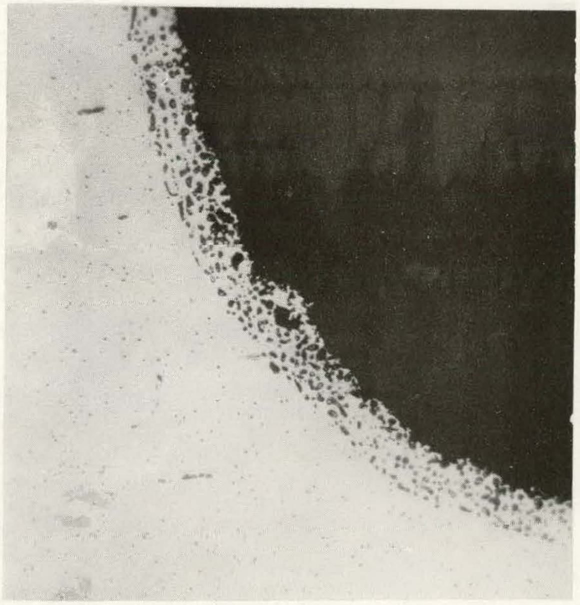

After Heating

SLIDE 14

^{242}Cm-EXPOSED 304L STAINLESS STEEL SPACER

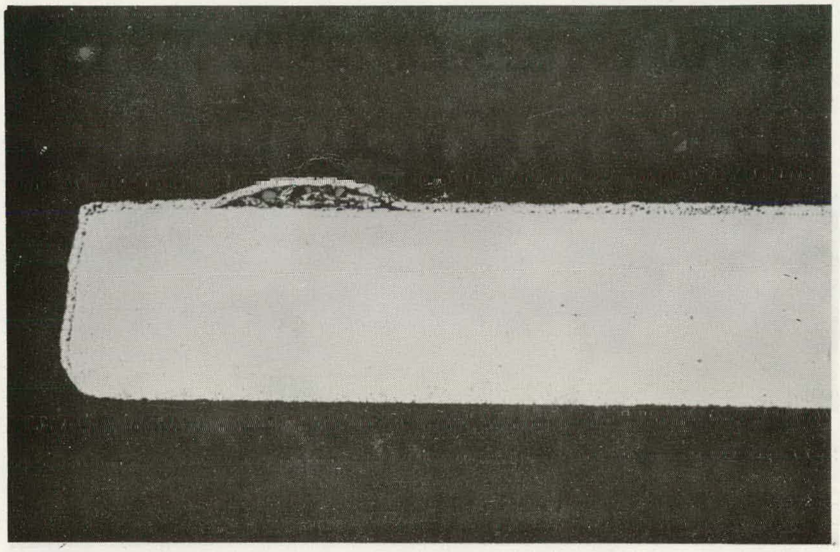

200 μm

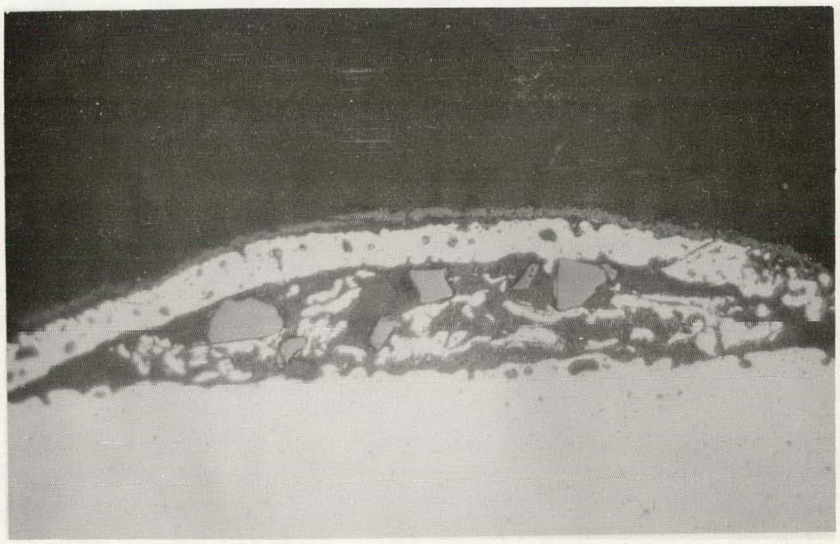

40 μm

SLIDE 15

Pt-10% Rh INNER CAPSULE FOR ^{252}Cf SOURCE (SCHEMATIC)

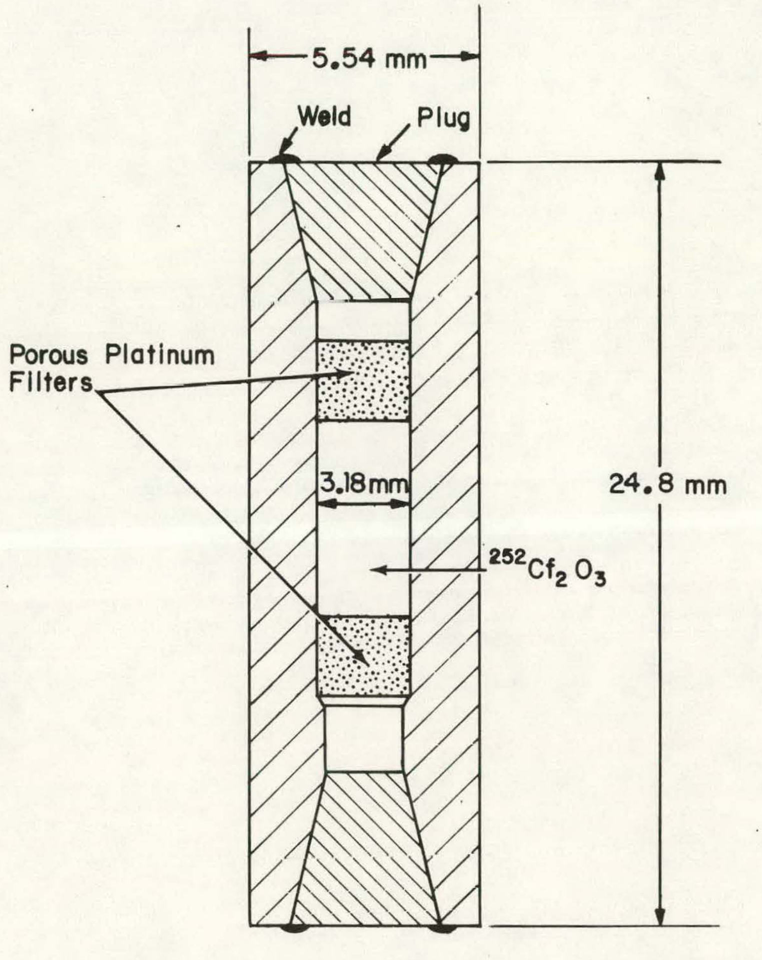

SLIDE 16

CONCENTRATION OF IMPLANTED HELIUM AND LATTICE DISPLACEMENTS IN CAPSULE SURFACE ADJACENT TO ^{252}Cf OXIDE DEPOSIT (APPROXIMATE)

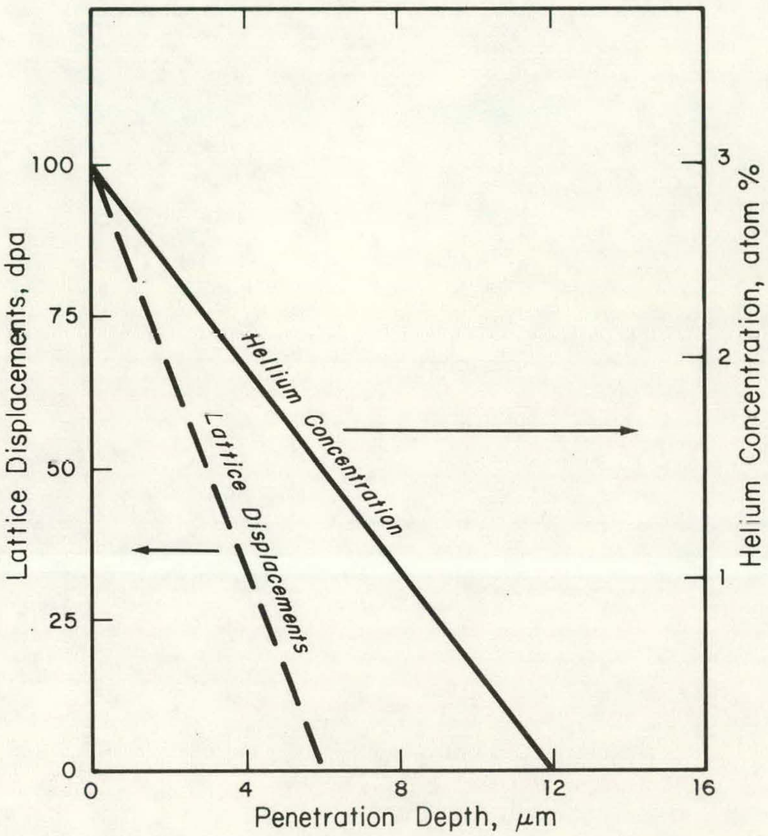

SLIDE 17

SURFACE BLISTERS AT VARIOUS DISTANCES FROM BOTTOM FILTER IN ^{252}Cf-CONTAINING Pt-10% Rh CAPSULE

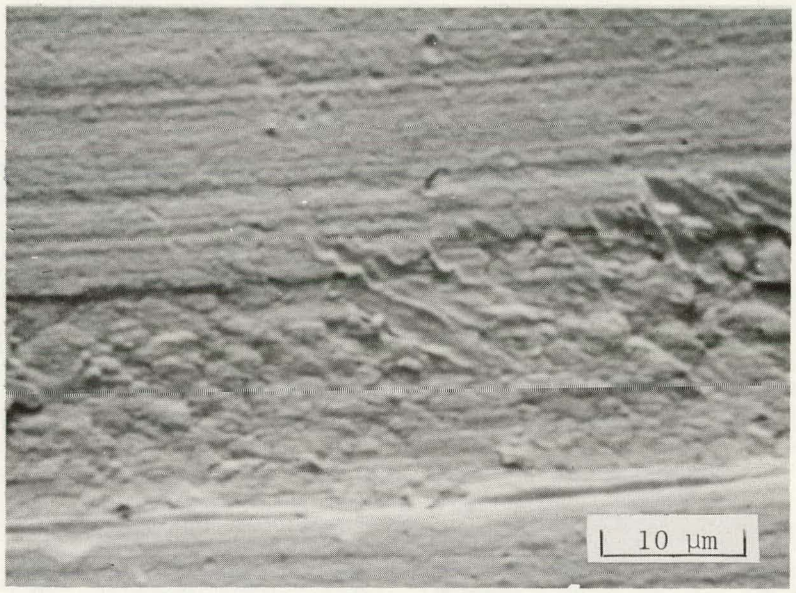

a. No Blisters Under Filter

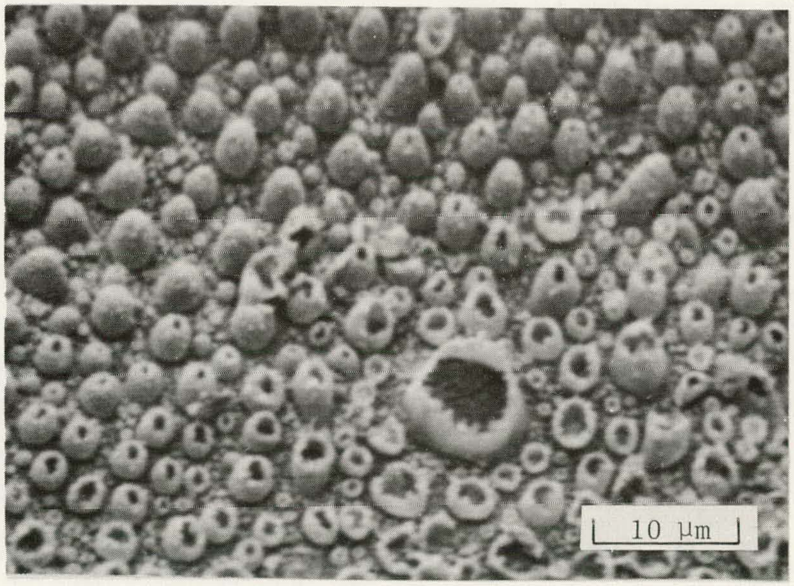

b. Circular Blisters Close to Filter

SLIDE 18

SURFACE BLISTERS AT VARIOUS DISTANCES FROM BOTTOM FILTER IN ^{252}Cf-CONTAINING Pt-10% Rh CAPSULE (CON'T)

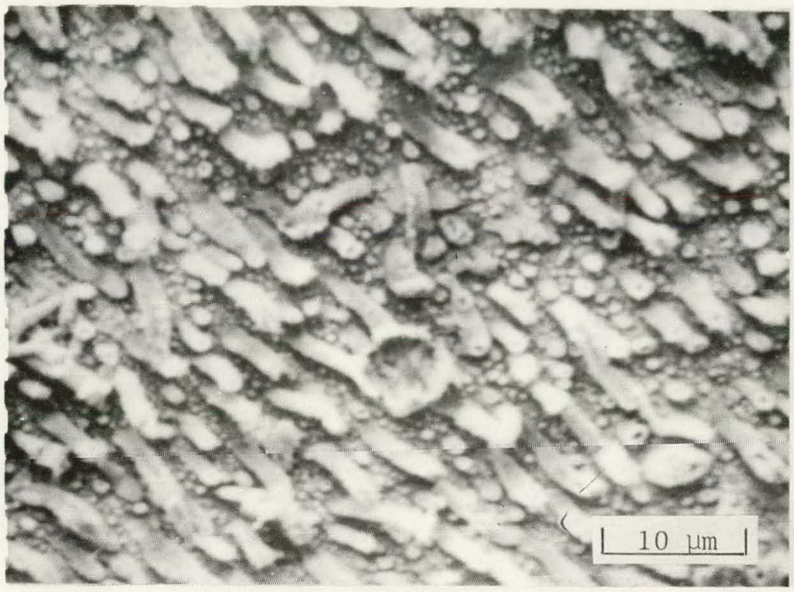

c. Laterally Elongated Blisters at Intermediate Distance from Filter

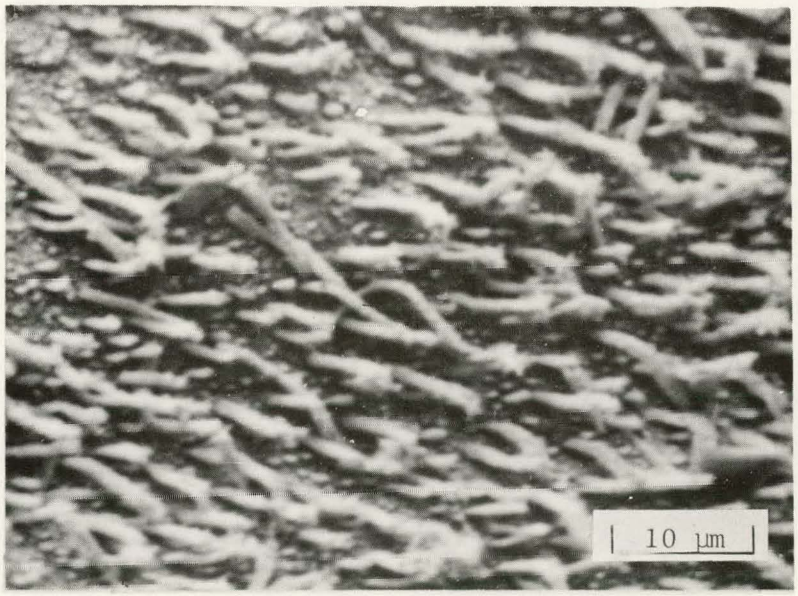

d. Vertically Elongated Blisters Far from Filter

SLIDE 19

COLUMNAR ARRAY OF LATERALLY ELONGATED
BLISTERS NEAR BOTTOM FILTER

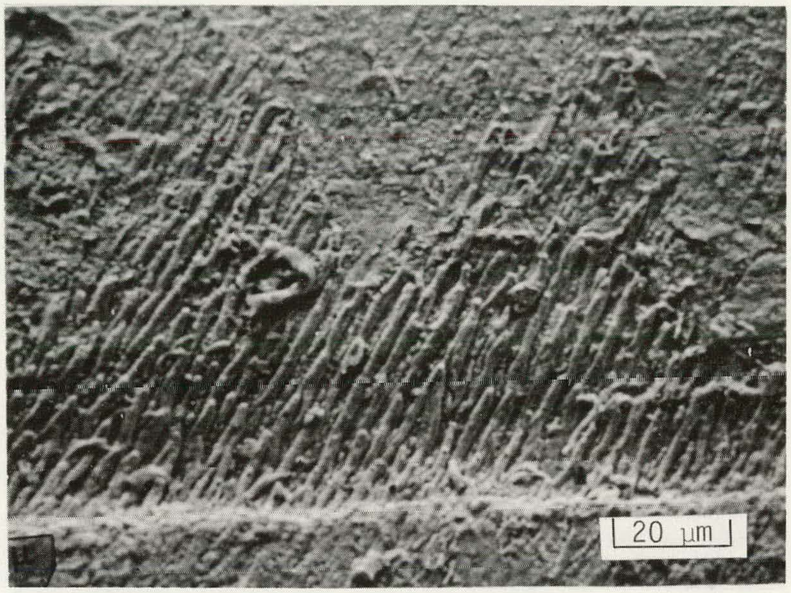

SLIDE 20

CIRCULAR AND LATERALLY ELONGATED BLISTERS
NEAR TOP FILTER

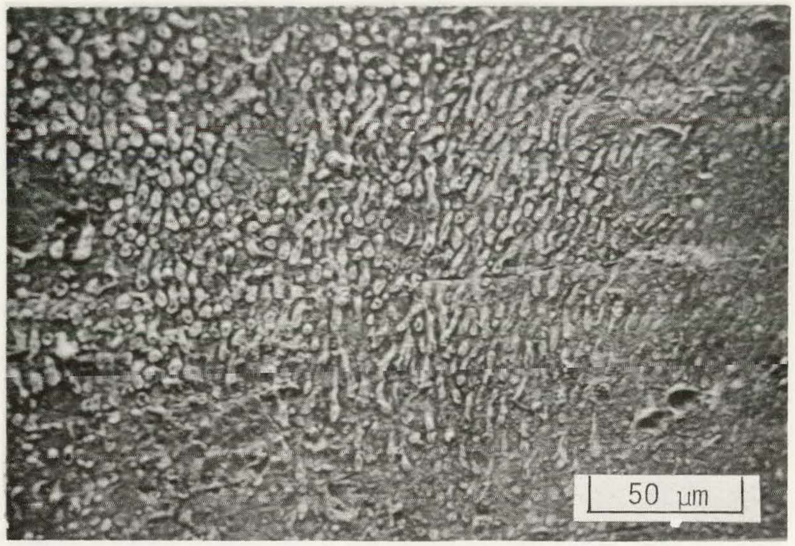

a. Interrelated Pattern of Circular and Laterally Elongated Blisters

b. Columnar Array of Laterally Elongated Blisters Showing Definite Spacing

SLIDE 21

SPALLING OF BLISTERED SURFACE NEAR BOTTOM FILTER OF ^{252}Cf-CONTAINING Pt-10% Rh CAPSULE

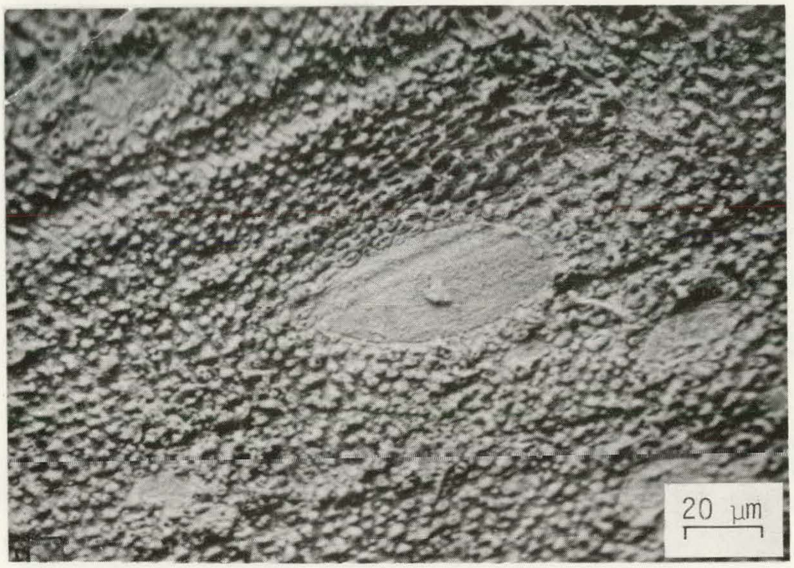

a. Spalling of Blistered Surface

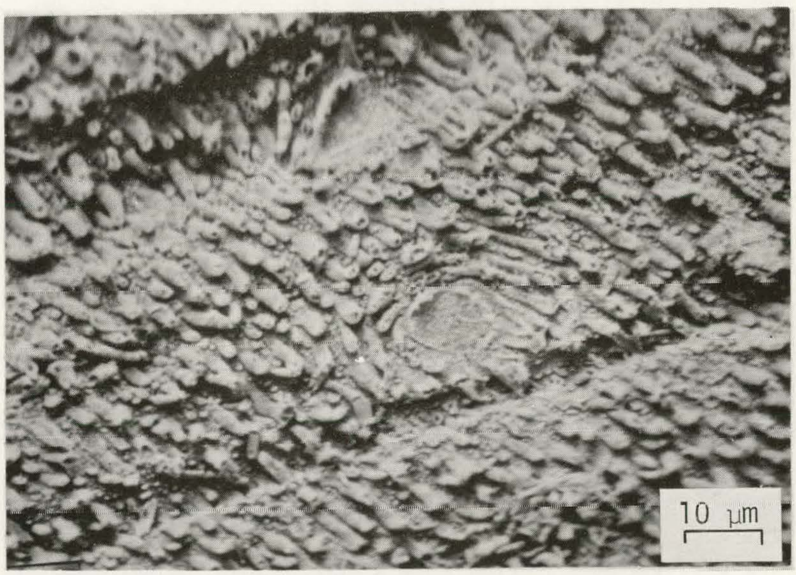

b. Growth Pattern of Laterally Elongated Blisters Around Spalled Area

SLIDE 22

IRREGULARITIES ON BLISTERED SURFACES NEAR BOTTOM FILTER OF ^{252}Cf-CONTAINING Pt-10% Rh CAPSULE

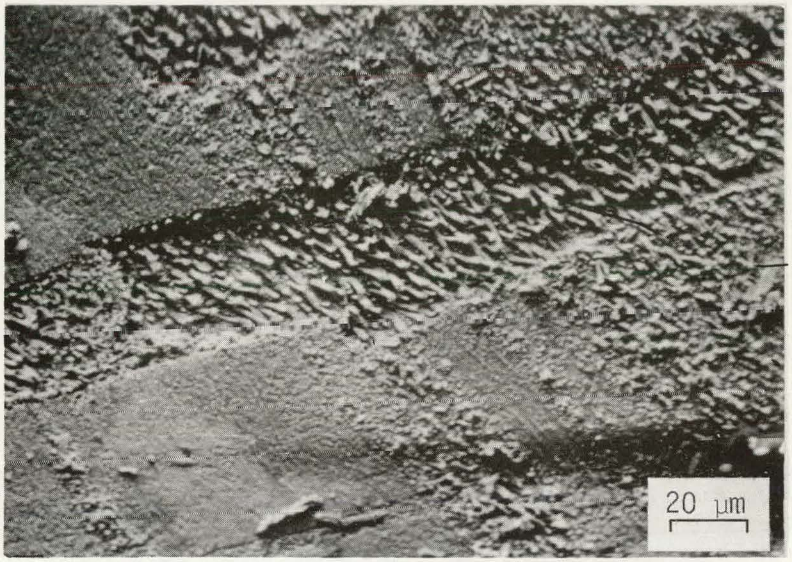

a. Abrasion of Blistered Surface

b. Shadowing of Blistered Surface by Protrusion

SLIDE 23

CONCEPTUAL MODEL FOR HELIUM BLISTER FORMATION ON SURFACE EXPOSED TO ^{252}Cf ALPHA PARTICLES AND FISSION FRAGMENTS

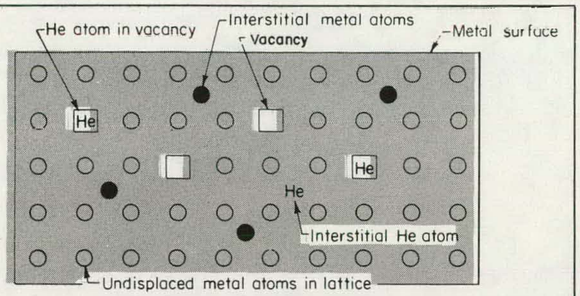

1. Vacancies and interstitial metal atoms are formed by fission fragments displacing metal atoms in lattice. Alpha particles deposit as He atoms in lattice. Volumetric expansion of surface layer restrained by attachment to underlying metal generates lateral compressive stress in surface layer.

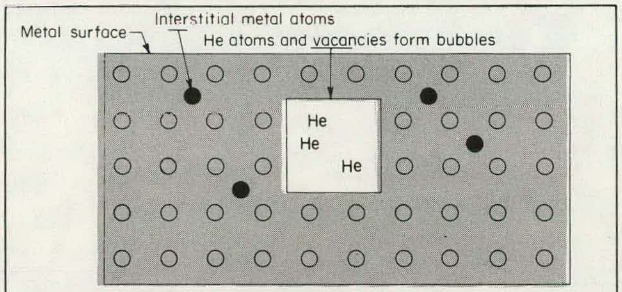

2. Helium atoms and vacancies coalesce into subsurface gas bubbles.

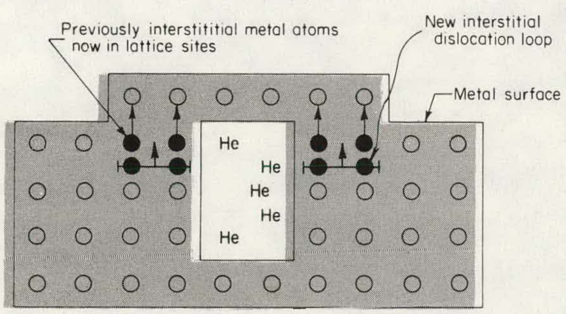

3. Interstitial metal atoms deposit in dislocation loops preferentially oriented parallel to surface by lateral compressive stress. Loop glides to surface displacing layer of atoms to form blister walls. New interstitial loop forms.

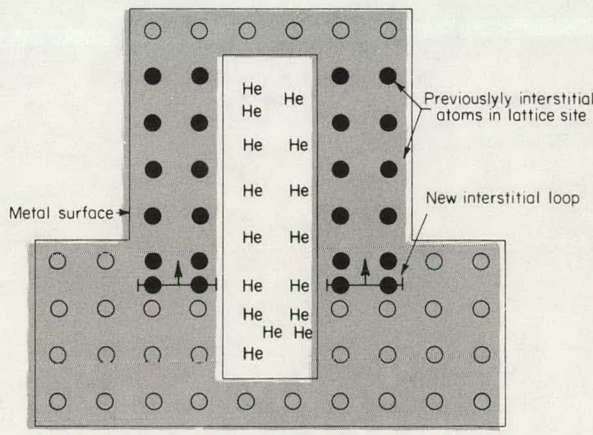

4. Repeated displacement of surface layers extends blister wall vertically.

SLIDE 24

INNER SURFACE OF ^{252}Cf-CONTAINING Pt-10% Rh CAPSULE AFTER HEATING AT 1000°C FOR 6000 HR

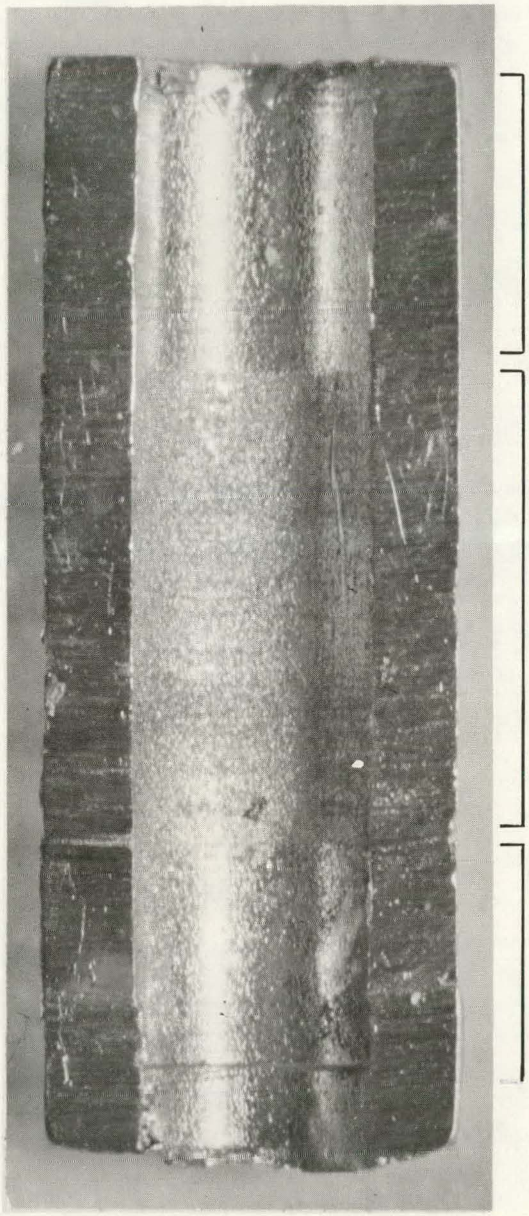

SLIDE 25

SURFACES OF ^{252}Cf-CONTAINING Pt-10% Rh CAPSULE AFTER HEATING AT 1000°C FOR 6000 HOURS

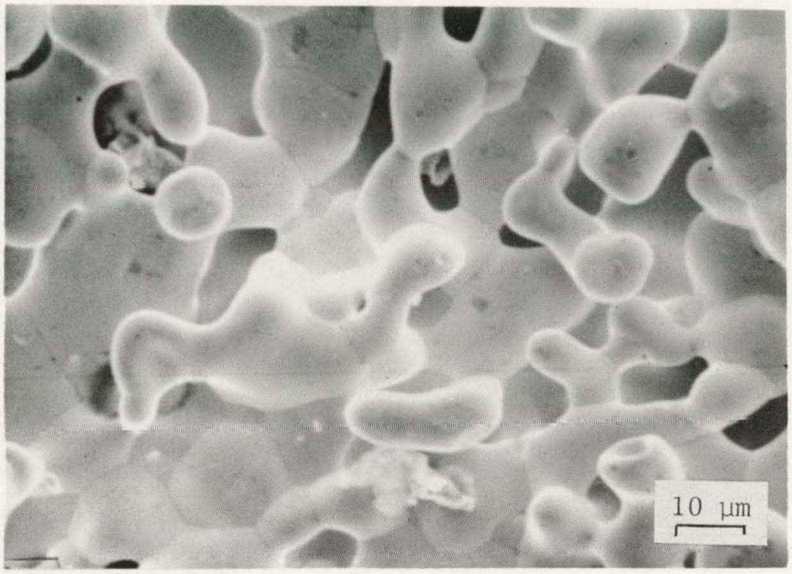

a. In ^{252}Cf-Containing Region Above Bottom Filter

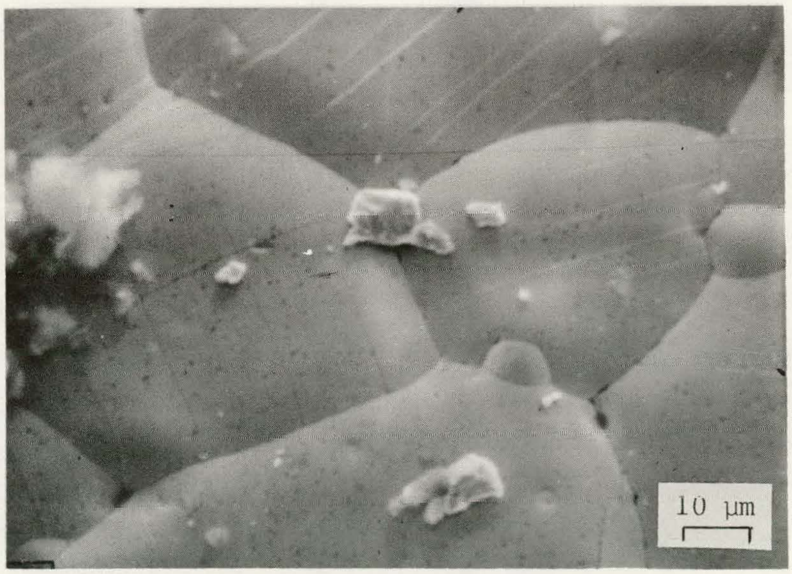

b. Under Bottom Filter

SLIDE 26

SURFACES OF GLASS SPECIMENS EXPOSED TO ^{242}Cm SOLUTIONS

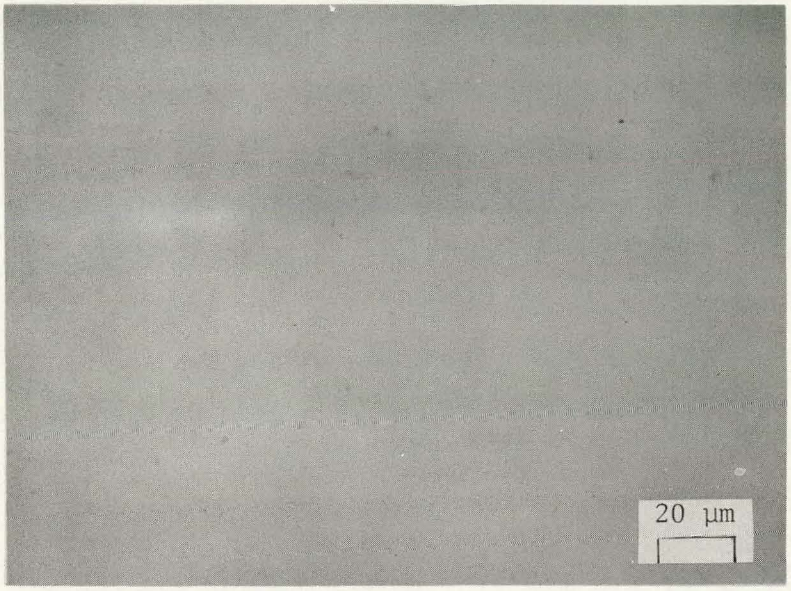

a. Soda-Lime Glass

b. Borosilicate Glass

SLIDE 27

SURFACES OF PLATINUM SPECIMEN EXPOSED TO ^{242}Cm SOLUTIONS

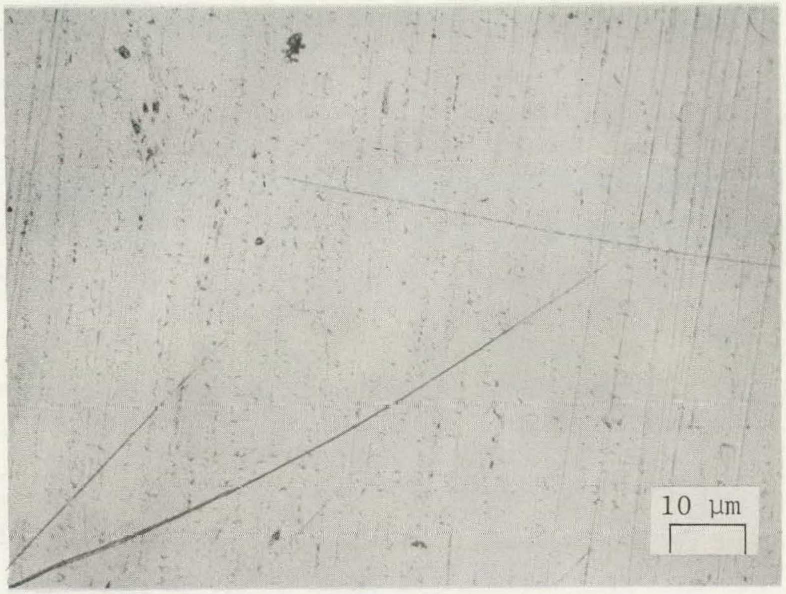

a. Exposed Specimen

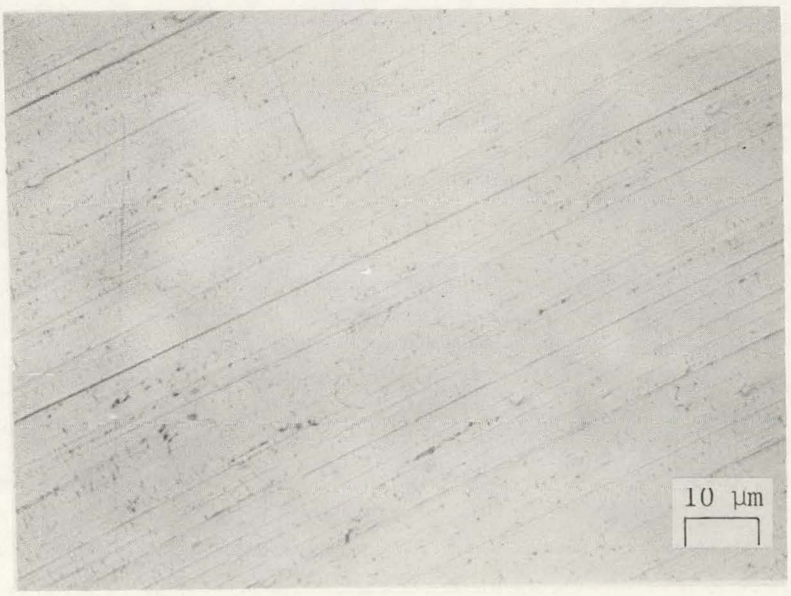

b. Unexposed Blank

SLIDE 28

SURFACES OF GLASS SPECIMENS EXPOSED TO ^{242}Cm SOLUTIONS AND REACTED WITH CONCENTRATED HNO_3

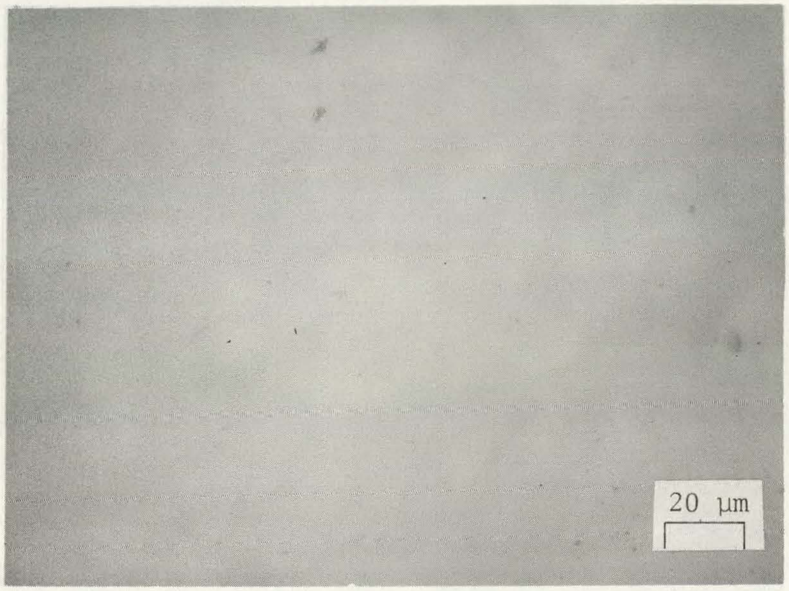

a. Soda-Lime Glass

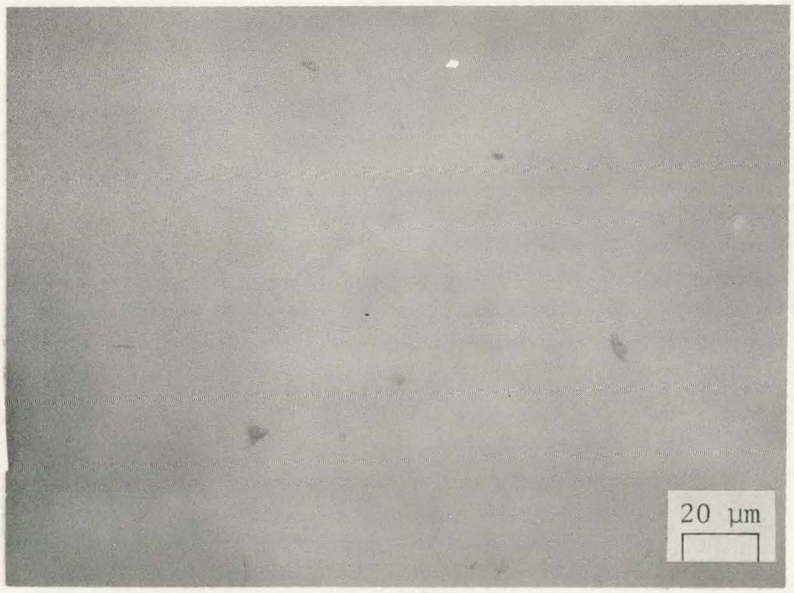

b. Borosilicate Glass

SLIDE 29

SURFACES OF GLASS SPECIMENS EXPOSED TO ^{242}Cm SOLUTIONS AND REACTED WITH 6N HCl

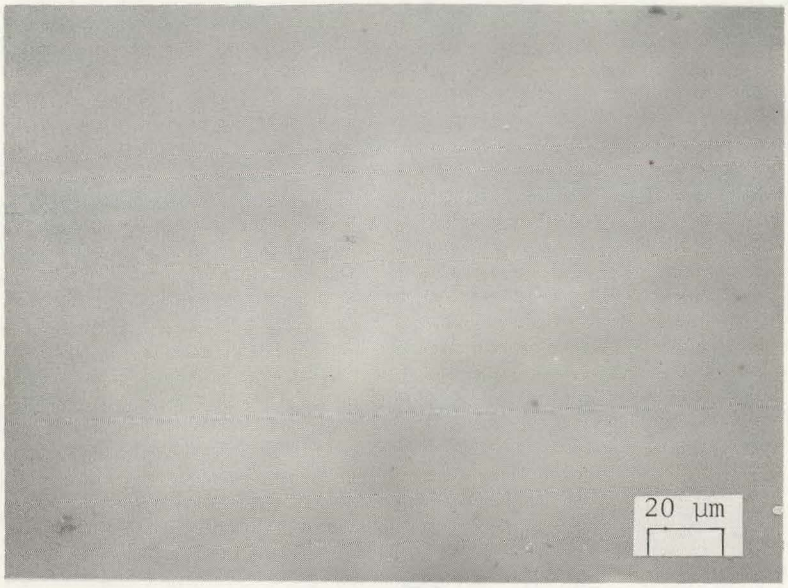

a. Soda-Lime Glass

b. Borosilicate Glass

SLIDE 30

SURFACES OF GLASS SPECIMENS EXPOSED TO ^{242}Cm SOLUTIONS AND REACTED WITH AQUA REGIA

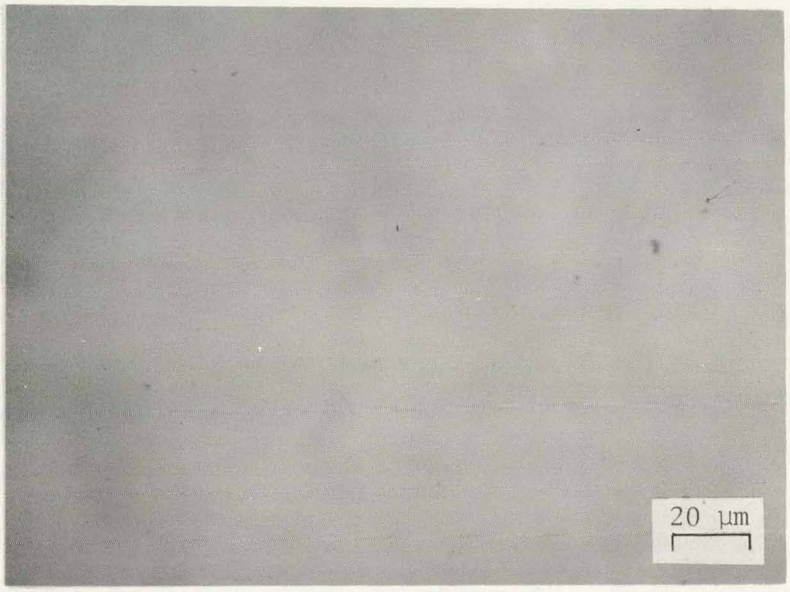

a. Soda-Lime Glass

b. Borosilicate Glass

SLIDE 31

SURFACES OF GLASS SPECIMENS EXPOSED TO ^{242}Cm SOLUTIONS AND REACTED WITH 6N KOH

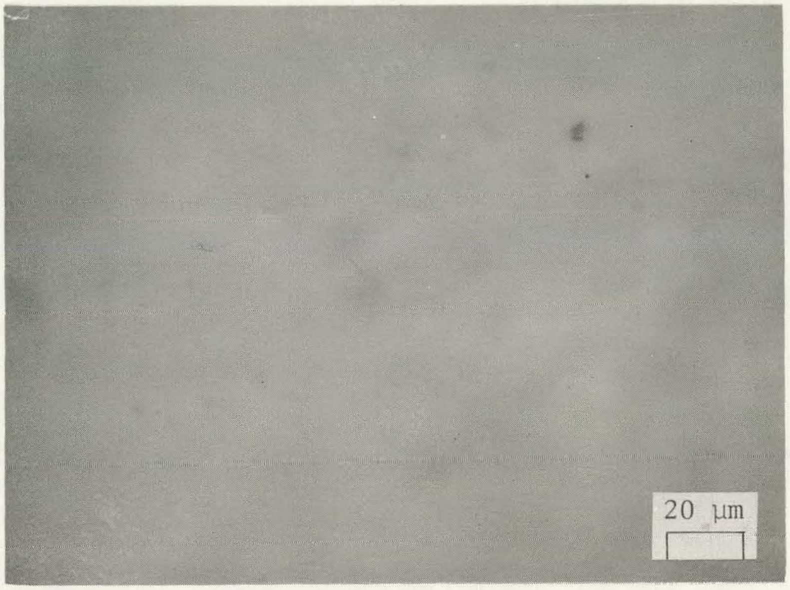

a. Soda-Lime Glass

b. Borosilicate Glass

SLIDE 32A

SURFACES OF GLASS SPECIMENS EXPOSED TO ^{242}Cm SOLUTIONS AND REACTED WITH 5% HF

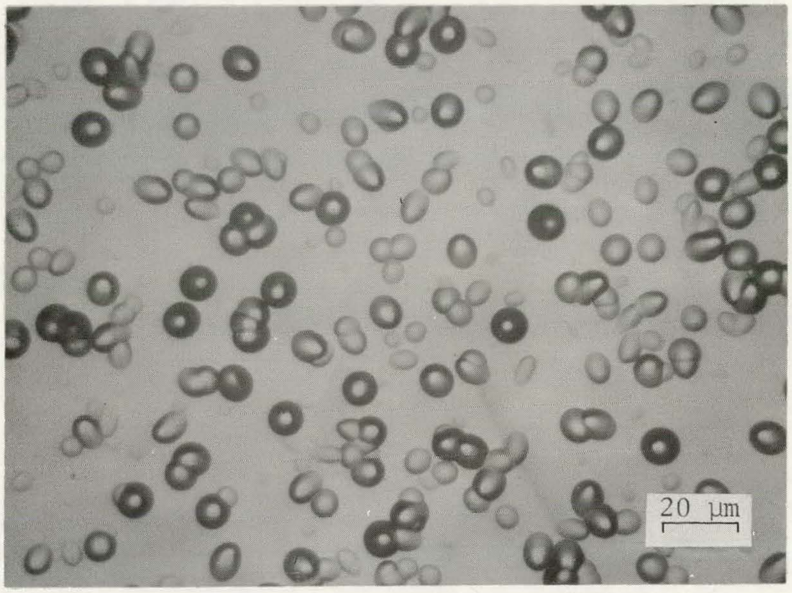

a. Soda-Lime Glass

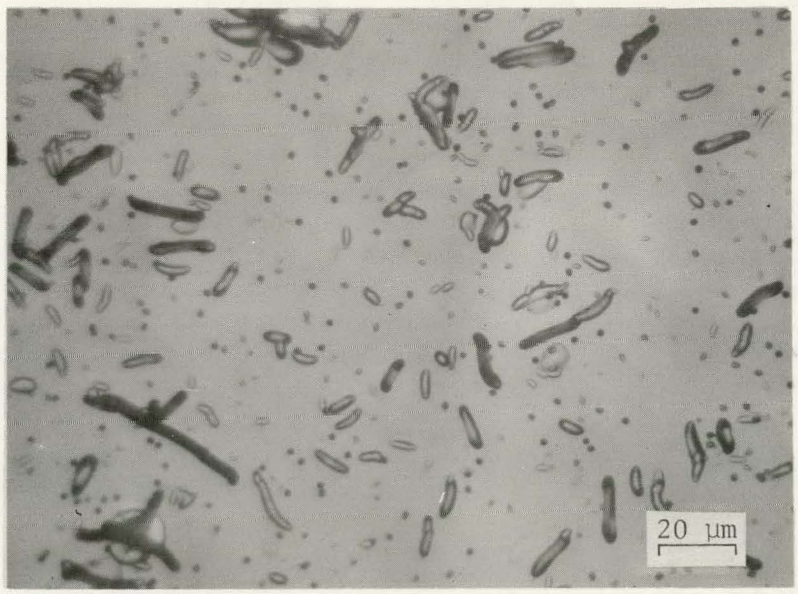

b. Borosilicate Glass

SLIDE 32B

SURFACES OF GLASS SPECIMENS EXPOSED TO ^{242}Cm SOLUTIONS AND REACTED WITH 5% HF

a. Soda-Lime Glass

b. Borosilicate Glass

SLIDE 33

SURFACES OF PLATINUM SPECIMEN EXPOSED TO ^{242}Cm
AND REACTED WITH AQUA REGIA

a. Exposed Specimen

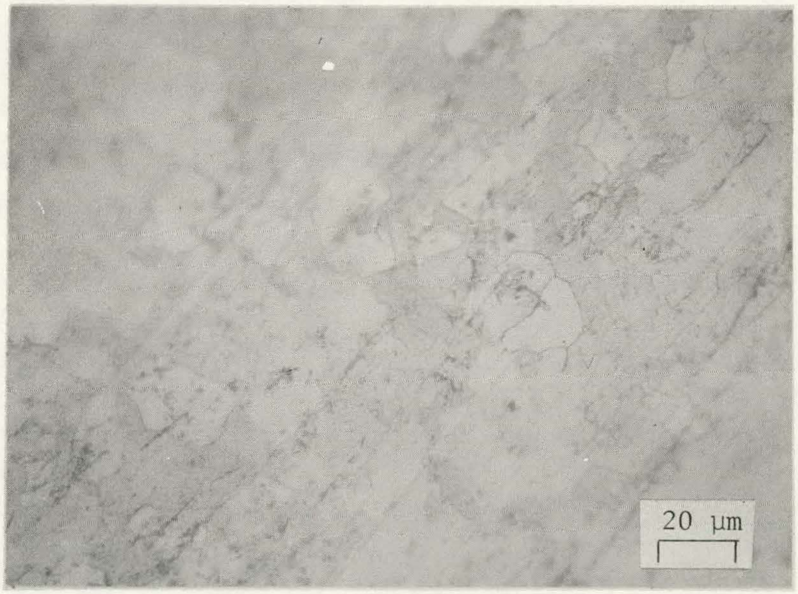

b. Unexposed Blank

SLIDE 34

SURFACES OF SODA-LIME GLASS SLIDE EXPOSED TO ^{252}Cf SOLUTION

a. Exposed Area

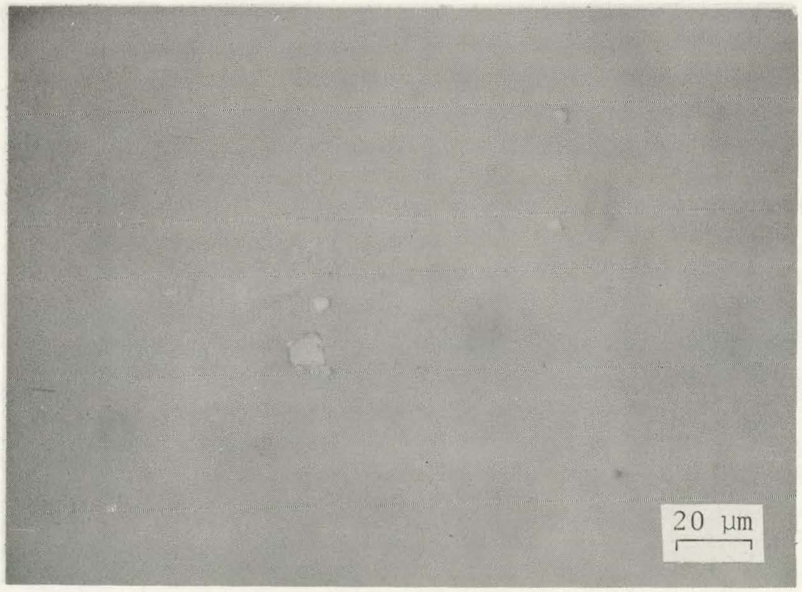

b. Unexposed Area

SLIDE 35

SURFACE OF SODA-LIME GLASS SLIDE EXPOSED TO ^{252}Cf SOLUTION AND REACTED WITH CONCENTRATED HNO_3

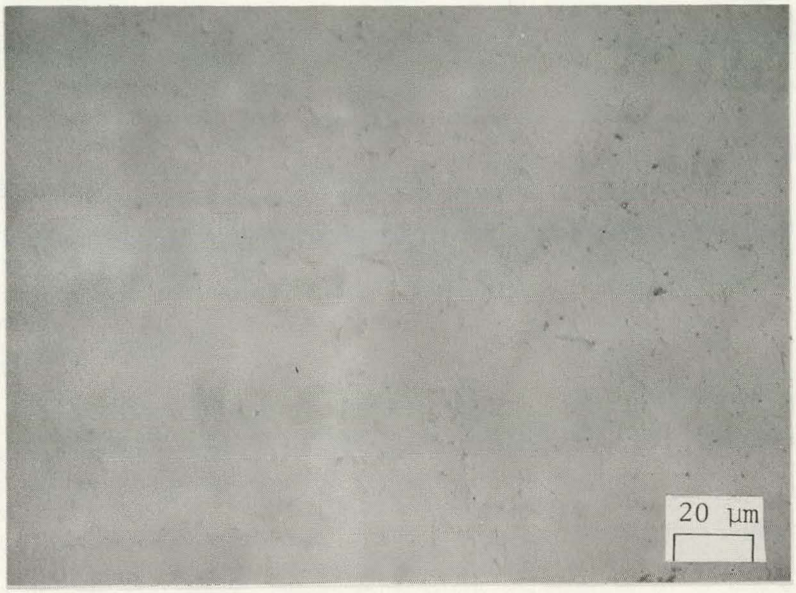

a. Exposed Area

b. Unexposed Area

SLIDE 36

SURFACE OF SODA-LIME GLASS SLIDE EXPOSED TO ^{252}Cf SOLUTION AND REACTED WITH 6N KOH

SLIDE 37

SURFACES OF SODA-LIME GLASS SLIDE EXPOSED TO ^{252}Cf SOLUTION AND REACTED WITH 5% HF (1 MIN)

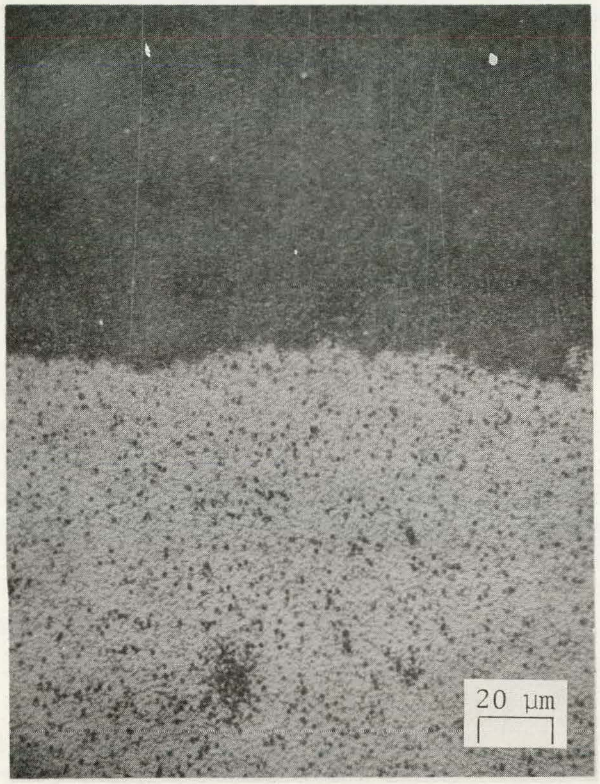

a. Interface Between Exposed and Unexposed Areas

b. Unexposed Area

SLIDE 38

SURFACES OF SODA-LIME GLASS SLIDE EXPOSED TO ^{252}Cf SOLUTION AND REACTED WITH 5% HF (5 MIN)

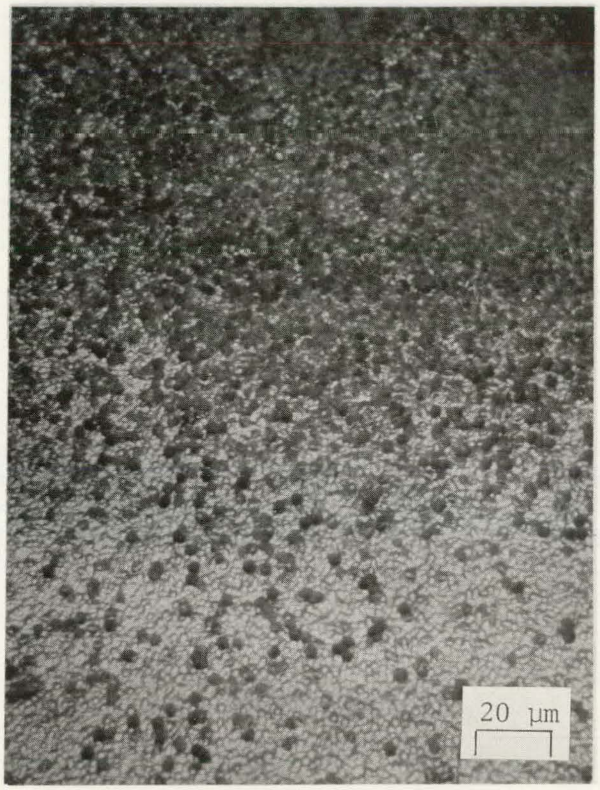

a. Interface Between Exposed and Unexposed Areas

b. Uncxposed Area

SLIDE 39

SURFACES OF SODA-LIME GLASS SLIDE EXPOSED TO ^{252}Cf SOLUTION AND REACTED WITH 5% HF (15 MIN)

a. Exposed Area

b. Interface Area

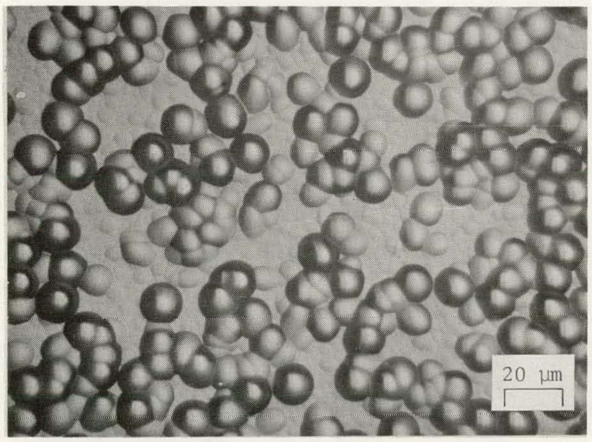

c. Near Interface Area

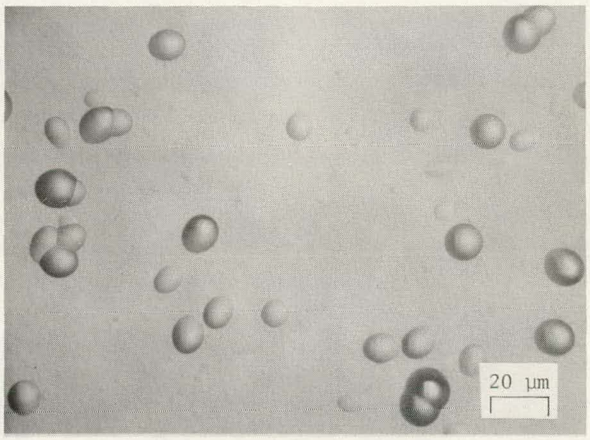

d. Unexposed Area

SLIDE 40

SURFACES OF SODA-LIME GLASS SLIDE EXPOSED TO ^{252}Cf SOLUTION AND REACTED WITH 5% HF (1 HR)

a. Exposed Area

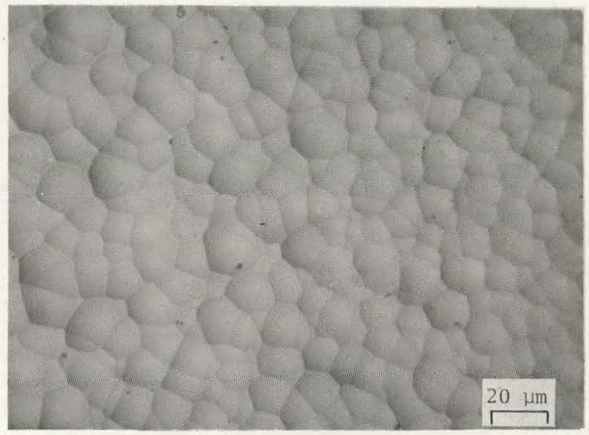

b. Interface Area

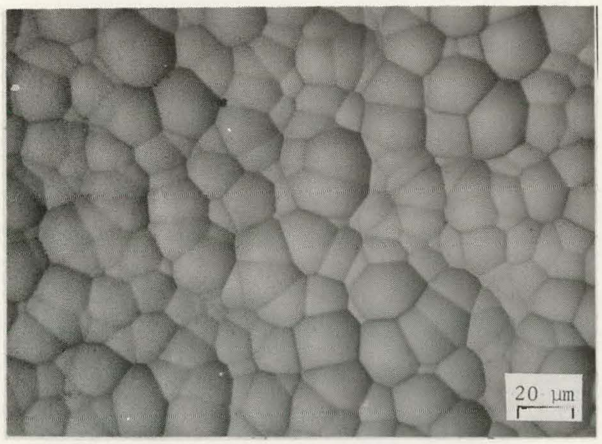

c. Near Interface Area

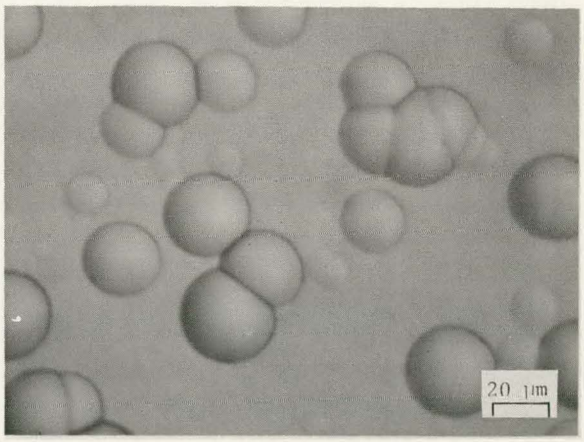

d. Unexposed Area

SLIDE 41

EFFECT OF STORAGE TIME ON RECOVERY OF ^{252}Cf FROM SHIPPING CONTAINERS

Date Loaded	*^{252}Cf Loaded, mg*	*Date Recovered*	*Residual ^{252}Cf On Container, μg*
10/1/71	7.25	11/10/71	30.5 (11/17/71)
10/1/71	7.20	10/13/71	20.4 (10/18/71)
10/1/71	7.14 (4.12)*	1/8/74	11.6 (1/8/74)

* Decayed to recovery date